HHS Public Access

Author manuscript

J Immunol. Author manuscript; available in PMC 2019 June 01.

Published in final edited form as:

J Immunol. 2018 June 01; 200(11): 3840–3856. doi:10.4049/jimmunol.1601317.

Farnesyltransferase Inhibition Exacerbates Eosinophilic Inflammation and Airway Hyperreactivity in Mice with Experimental Asthma: *The Complex Roles of Ras GTPase and Farnesylpyrophosphate in Type-2 Allergic Inflammation*

Jennifer M. Bratt[1,2], **Kevin Y. Chang**[1], **Michelle Rabowsky**[1], **Lisa M. Franzi**[1,2], **Sean P. Ott**[1,2], **Simone Filosto**[1,2,3], **Tzipora Goldkorn**[1,2,3], **Muhammad Arif**[1,2], **Jerold A. Last**[1,2], **Nicholas J. Kenyon**[1,2], and **Amir A. Zeki**[1,2,**]

[1]Division of Pulmonary, Critical Care, and Sleep Medicine, Department of Internal Medicine, University of California, Davis

[2]Department of Internal Medicine, Center for Comparative Respiratory Biology and Medicine (CCRBM), University of California, Davis

[3]Department of Internal Medicine, Respiratory Signal Transduction, Genome and Biomedical Sciences Facility (GBSF), University of California, Davis

Abstract

Ras, a small GTPase protein, is thought to mediate Th2-dependent eosinophilic inflammation in asthma. Ras requires cell membrane association for its biological activity and this requires the post-translational modification of Ras with an isoprenyl group by farnesyltransferase (FTase) or geranylgeranyltransferase (GGTase). We hypothesized that inhibition of FTase using FTI-277 would attenuate allergic asthma by depleting membrane-associated Ras. We used the ovalbumin (OVA) mouse model of allergic inflammation and human airway epithelial (HBE1) cells to determine the role of FTase in inflammatory cell recruitment. BALB/c mice were first sensitized then exposed to 1% OVA aerosol or filtered air, and half were injected daily with FTI-277 (20 mg/kg/day). Treatment of mice with FTI-277 had no significant effect on lung membrane-anchored Ras, Ras protein levels, or Ras GTPase activity. In OVA-exposed mice, FTI-277 treatment increased eosinophilic inflammation, goblet cell hyperplasia, and airway hyperreactivity. Human bronchial epithelial (HBE1) cells were pre-treated with 5, 10, or 20 μM FTI-277 prior to and during 12-hour IL13 (20 ng/mL) stimulation. In HBE1 cells, FTase inhibition with FTI-277 had no significant effect on IL13-induced STAT6 phosphorylation, eotaxin-3 peptide secretion, or Ras translocation. However, addition of exogenous FPP unexpectedly augmented IL13-induced STAT6 phosphorylation and eotaxin-3 secretion from HBE1 cells without affecting Ras translocation. Pharmacological inhibition of FTase exacerbates allergic asthma suggesting a protective role for FTase or possibly Ras farnesylation. FPP synergistically augments epithelial eotaxin-3 secretion indicating a novel Ras-independent farnesylation mechanism or direct FPP effect that promotes epithelial eotaxin-3 production in allergic asthma.

**Corresponding Author: Amir A. Zeki, MD, MAS, University of California, Davis, Genome and Biomedical Sciences Facility (GBSF), 451 East Health Sciences Drive, Room 6517, Davis, California 95616, aazeki@ucdavis.edu, Phone: (530) 754-5469, Fax: (530) 752-8632.

Keywords

Farnesyltransferase inhibition; asthma; airway inflammation; airway hyperreactivity; Ras GTPase; FTI-277; farnesylpyrophosphate; farnesyl diphosphate; eosinophils; isoprenylation; farnesylation

INTRODUCTION

Asthma is a chronic allergic disease affecting 300 million adults and children worldwide[1]. While conventional treatments such as inhaled corticosteroids (ICS) can reduce exacerbation rates in patients with mild or moderate asthma, they do not alter the course of the disease and have limited efficacy in some severe asthma patients. A better understanding of asthma pathogenesis can lead to novel therapies that better target specific subpopulations of asthmatics who do not respond to conventional therapies.

The mevalonate (MA) metabolic cascade is a ubiquitous anabolic biochemical pathway essential for cellular function in both prokaryotic and eukaryotic organisms. Mevalonate is the immediate product of 3-hydroxy-3-methyl-glutaryl-CoA reductase (HMGCR), the rate-limiting step in cholesterol biosynthesis in the MA pathway (Figure 1). Mevalonate is further metabolized into the lipid isoprenoid intermediates farnesylpyrophosphate (FPP) and geranylgeranylpyrophosphate (GGPP), where FPP can also converted to GGPP or squalene, an important lipid precursor of cholesterol[2] (Figure 1).

HMGCR inhibitors, a.k.a. statins, inhibit the synthesis of the isoprenoids and cholesterol by directly inhibiting HMGCR which depletes the pool of available MA. We and others showed that statins reduce murine allergic airway inflammation, attenuate airway hyperreactivity (AHR), and inhibit early hallmarks of airway remodeling[3–5] such as goblet cell hyperplasia and arginase protein expression and enzyme activity[6,7]. While we recognize the pleiotropic effects of statins and their potential off-target effects[8–10], the anti-inflammatory statin effects in the ovalbumin (OVA) mouse model and in human airway epithelial cells appear to occur primarily via inhibition of HMGCR[6,7,11].

The prenyltransferases including farnesyltransferase (FTase) and geranylgeranyltransferase (GGTase I/II) catalyze the attachment of farnesyl or geranylgeranyl groups to Ras and Rho/Rab family GTPases, respectively, a reaction collectively known as isoprenylation[12] (Figure 1). The FTase enzyme recognizes FPP and also binds the CaaX box motif located on the C-terminus of proteins such as Ras GTPase, catalyzing the formation of the thioester linkage between the cysteine of the CaaX motif and the C1 of the FPP molecule[13]. These are critical post-translational protein modifications that allow Ras GTPases to anchor in cell membranes in order to affect signal transduction[14].

While statins deplete MA and downstream FPP and GGPP to *indirectly* reduce farnesylation and geranylgeranylation events, the FTase inhibitors (FTI) and GGTase inhibitors (GGTI) *directly* block farnesylation and geranylgeranylation, respectively[2,13]. Therefore, it is important to determine which sub-arm of the MA pathway (the isoprenoid (FTase/Ras family, GGTase-I/Rho family, GGTase-II/Rab), or sterol (squalene/cholesterol) parts) mimics the beneficial statin effect observed in asthma.

RhoA activity is elevated in allergic asthma[15–17], and GGTase-I inhibition mitigates eosinophilic inflammation and AHR in a murine model of allergic inflammation[16–18]. Our study focuses on the FTase enzyme (Figure 1) because it promotes Ras GTPase signaling in cells, a process thought to be necessary for eosinophilic inflammation and the development of helper T-cell type-2 (Th2) /type 2 allergic asthma[19–22].

In animal models of allergic asthma, Ras modulates T-cell-dependent allergic inflammation, and eosinophilic trafficking/transmigration[19,21–23]. Previous work by Myou *et al* using dominant negative Ras constructs to nullify Ras activity showed that Ras was necessary for this Th2 induction in mice[19]. However, despite the apparent role of Ras in allergic inflammation, no one has investigated the contributions of FTase to asthma pathogenesis. To further understand the mechanism of the statin-dependent anti-inflammatory effect in asthma[6,24,25], we investigated the role of Ras protein farnesylation via the actions of FTase in normal and inflamed murine lungs, and in human airway epithelial cells.

In this study, we hypothesized that pharmacological inhibition of FTase activity would 1) reduce Ras membrane association, 2) reduce overall Ras GTPase activity, and 3) inhibit indicators of allergic type-2 inflammation (eosinophilic airway inflammation, lung STAT6 activation, goblet cell metaplasia/hyperplasia, AHR). To test this hypothesis, we investigated the therapeutic potential of FTase inhibitor FTI-277 *in vivo* using the ovalbumin (OVA) mouse model, and examined its effect on Ras membrane localization and enzyme activity in lung tissues. We then examined the effect of FTI-277 on IL13-dependent STAT6 activation and eotaxin-3 (CCL26) production *in vitro* using HBE1 human bronchial epithelial cells to examine the mechanism in a single cell type relevant to type 2 (Th2) asthma. Downstream of the IL13 receptor, a key Th2 effector molecule in asthma, STAT6 is the primary transcription factor for eotaxin-1, -2, and -3 gene expression. Eotaxin-3 has clinical relevance in IL13-mediated inflammation and human severe asthma[26,27], and is one of the main chemokines associated with Th2-high inflammation and airway eosinophilia in asthma[26]

To our surprise, the results of these experiments unexpectedly supported the null hypothesis; that systemic treatment of allergic mice with FTI-277 further *exacerbated* eosinophilic airway inflammation, worsened AHR, and increased goblet cell hyperplasia. These results further compelled us to conduct *in vitro* cell culture experiments which allowed us to isolate drug effect(s) in a single cell type to better understand our *in vivo* results. Our cell culture experiments were necessary for three reasons: 1) Given the complexity of Ras and FTase biology in the intact animal host (assayed as whole lung homogenates), results of FTase antagonism *in vivo* can be difficult to interpret when using pharmacologic inhibition alone, 2) Evaluating Ras and FTase mechanisms in HBE1 cells is important given that the airway epithelium plays a central role in human asthma pathogenesis (i.e. elucidating the contribution of epithelial FTase inhibition to allergic inflammation), and 3) Understanding drug effects on airway epithelial cells has direct implications for the development of inhaler therapies.

While treatment with FTI-277 inhibited Ras farnesylation, and therefore, depleted membrane-anchored Ras in HBE1 cells at shorter treatment durations (i.e. 30 minutes), treatment of HBE1 cells with FTI-277 for longer durations (i.e. 72 hours) had no significant

effect on Ras membrane/cytosol translocation, IL13-induced STAT6 activation, or eotaxin-3 peptide secretion. Interestingly, exogenous treatment of HBE1 cells with the isoprenoid FPP further augmented IL13-induced STAT6 phosphorylation and eotaxin-3 secretion beyond the activating effects of IL13 alone.

Our findings provide further evidence that the MA cascade plays an important role in asthma pathogenesis, and contribute to our understanding of the interrelated roles of Ras, FTase, and FPP in allergic inflammation. Our data suggest that FTase and Ras GTPase have complex and possibly protective roles in normal physiology and asthma pathogenesis. FPP itself markedly increases eotaxin-3 production in human airway epithelial cells, an unexpected finding worthy of further study. Excess airway FPP from cellular sources may play a role in perpetuating eosinophilic airway inflammation in asthma.

METHODS

Drug Inhibitor

The farnesyltransferase (FTase) inhibitor FTI-277 and farnesylpyrophosphate (FPP) were purchased from Sigma-Aldrich (St. Louis, MO). FTI-277 is a Ras CaaX peptidomimetic (Figure 1) with an IC_{50} of 50 nM (Sigma-Aldrich, St. Louis, MO). FTI-277 was dissolved in dimethyl sulfoxide (DMSO) at a concentration of 10 mM and stored at −20°C for future application. The 10 mM FTI-277 solution was further diluted using sterile phosphate buffered saline (PBS) at a pH 7.4 for all experiments. For *in vivo* experiments, the FTI-277 final concentration was 2.5 mg/mL (equivalent to a dose of 20 mg/kg or 0.5 mg per mouse per day). FPP was initially dissolved in a solution of methanol and 10 mM ammonium hydroxide (NH_4OH) to a concentration of 1 μg/μL and stored at −20 °C. FPP was further diluted to the desired concentrations (5, 10, and 20 μM) in sterile PBS for use in cell culture experiments. The vehicle control for FPP was its chemical solvent methanol:NH_4OH (70:30). Previous experiments in our lab showed no evidence of cytotoxicity of this solvent in HBE1 cells using either MTT or Alamar blue assays.

Animals

Eight-week-old pathogen-free male BALB/c mice were purchased from Charles River Breeding Laboratories (Wilmington, MA). Mice were housed and cared for by the veterinary staff of the Animal Resource Services at the University of California, Davis, following institutional standards and regulations for animal care and use. All mice were maintained in a HEPA-filtered laminar flow cage rack with a 12-hour light/dark cycle with free access to water and food throughout the study and were routinely screened for health status. All procedures were performed following our Institutional Animal Care and Use Committee-approved protocol. Animal weights were measured prior to allergen sensitization and on days 1, 3, and 6 days post FTI-277 injections.

Drug Regimen and Ovalbumin Aerosol Exposures

Mice were sensitized by two intraperitoneal (i.p.) injections of 10 μg/0.1 mL ovalbumin (OVA) in PBS, pH 7.4 with alum adjuvant on Day 0 and 14. After sensitization, mice were

divided into four treatment groups as follows: OVA + PBS (n=6), OVA + FTI-277 (n=6), filtered air (FA) + PBS (n=4), and FA+ FTI-277 (n=4).

Starting on day 28 mice received daily i.p. injections of 20 mg/kg FTI-227 (equivalent to 0.5 mg per mouse per day), administered 30 minutes prior to OVA/filtered air (FA) exposures, for 14 days during the two-week OVA exposure period. OVA aerosol exposures began on day 28 and were performed using nebulizers and aerosol exposure chambers as described previously[28,29]. Briefly, OVA treatment groups were exposed to aerosol derived from 10 mL of 1% (w/v) OVA in PBS (for 30 min), three times a week over a duration of two weeks and for a total of 6 exposures (i.e. “6OVA”). Aerosol delivery was performed using a side-stream nebulizer (Invacare Corp., Elyria, Ohio) and air compressor (Invacare Corp., Sanford, Fla). Aerosol characterization was performed as described in Kenyon *et al.*[30].

Lung Physiology Measurements

Pulmonary function parameters were measured using a Buxco restrained whole body plethysmograph (Buxco Inc. Troy, NY). After the final OVA aerosol or FA exposure, mice were anesthetized and sedated using a dose of 0.5 mg/kg medetomidine (Dormitor; Orion Pharma, Espoo, Finland) and tiletamine-zolazepam (Telazol; Fort Dodge Laboratories, Fort Dodge, Iowa). The mice were then cannulated with a blunt-tipped tube for mechanical ventilation (MiniVent; Harvard Apparatus, Cambridge, MA) at a stroke volume of 200 μL and a frequency of 150 breaths/min.

Lung compliance (Cdyn, mL/cm H_2O) and total respiratory resistance (Rrs, cm H_2O*s/mL) were calculated at baseline, using 3-minute average values, and over a course of nebulized aerosols of saline and methacholine (MCh) dose response challenge (0, 0.5, 1.0, and 2.0 mg/mL), as described in detail previously by Zeki *et al.*[6].

Tissue Processing and BALF Inflammatory Cell Counts

Immediately after collection of lung physiology measurements, mice were sacrificed with an overdose of Beuthanasia-D (pentobarbital sodium and phenytoin sodium). Lungs were lavaged twice with 1 mL of PBS (pH 7.4) containing 1 mM phenylmethanesulfonylfluoride (PMSF) and 1:100 v/v protease inhibitor cocktail (Sigma-Aldrich, St. Louis, MO) and centrifuged at 325 *g*. Bronchoalveolar lavage fluid (BALF) supernatant was decanted and stored at −20 °C for multiplex cytokine profiling and albumin measurements. The cell pellet was re-suspended in AKC lysis buffer (0.15 M NH_4Cl, 1 mM $KHCO_3$, 0.1 mM EDTA), pH 7.3) to lyse red blood cells, then centrifuged and re-suspended in 0.5 mL PBS. The total live cell number from lavage was determined by Trypan Blue exclusion using a standard manual hemacytometer.

Single 100 μL aliquots from each of the cell suspensions were processed onto slides using a cytocentrifuge at 1,650 rpm for 7 min. Slides were stained with a Hema3 stain set per the manufacturer’s instructions (Fisher Scientific, Kalamazoo, Michigan). BALF cell percent differentials were determined by counting 10 fields under a 40X objective, based on morphological characteristics and staining profiles.

After performing lung lavage, the right bronchus of each lung was ligated using surgical suture. The right bronchus was severed distal to the ligation suture, and snap frozen at −80°C for future use. The remaining left lung was fixed *in situ* for histological evaluation at 20 cmH_2O with 1% paraformaldehyde (in PBS at pH 7.4) and processed for paraffin embedding as described in Zeki *et al.* 2010 [7].

Mouse Lung Tissue Homogenization and Fractionation

Lung homogenates were prepared from the right superior and middle lung lobes using isolation buffer (250 mM sucrose, 20 mM HEPES, pH 7.4, 2 mM EDTA, and 3 mM NaN_3) containing protease inhibitors (Protease Inhibitor (Sigma, 1:100), 1 mM PMSF, 1 mM Na_3VO_4, and 1 mM NaF) and Phosphatase Inhibitor (Sigma, 1:100). The lung tissue was homogenized by hand using a chilled dounce homogenizer. The resulting crude homogenates were centrifuged at 800 *g* for 5 min at 4°C. The supernatant was removed and total protein concentration was determined using the BCA Protein Assay (Pierce Biotechnology, Rockford, Ill).

Homogenates were diluted to 5 μg/μL and an aliquot reserved as “total” homogenate. A 200 μL aliquot of total homogenate was ultra-centrifuged at 30,000 *g* at 4°C for an additional 30 minutes to separate the cytosolic and membrane components. The supernatant from this step was collected (~200 μL) and referred to as the “cytosolic” fraction. The remaining pellet was re-suspended in 200 μL isolation buffer and referred to as the “membrane” fraction. All subcellular fractions were stored at −80°C.

Western Blot Analyses

SDS-PAGE electrophoresis was performed on the cytosolic and membrane fractions (30 μg total protein) under reducing conditions and transferred to a polyvinylidene difluoride (PVDF) membrane. The gel composition differed slightly for Ras as compared to other proteins, where a 12% gel was used for Ras and 10% for all other proteins. This facilitated better protein separation for Ras isoforms and the assessment of farnesylated versus unfarnesylated Ras. Membranes were probed using rabbit (anti-mouse) anti-Ras IgG (1:1,000; 100 μL; Cell Signaling Technology, Inc.), monoclonal anti-E-cadherin IgG (1:1,000; 0.1 μg/mL; BD Bioscience, San Jose, CA), anti-GAPDH IgG_1 (1:50,000; 200 μg/mL; Santa Cruz Biotechnology, Inc., Dallas, TX), rabbit anti-α-actinin IgG (1:1,000; Santa Cruz Biotechnology, Inc., Dallas, TX), and rabbit total- and phospho-STAT6 IgG (primary antibody 1:1,000; secondary antibody goat anti-rabbit 1:10,000) at 4°C followed by incubation in 40 ng/mL HRP-conjugated goat anti-rabbit IgG (Pierce Biotechnology, Rockford, IL) or HRP-conjugated goat anti-mouse IgG (R&D Systems, Minneapolis, MN) in 5% dry milk in 0.05% Tween in PBS (PBST). Bands were visualized using Western Lightning Plus-ECL substrate (PerkinElmer, Shelton, CT) and Image Reader LAS-4000 V2.1 (Fuji Photo Film Co., Cypress, CA) or the Konica SRX 101A Medical Film Processor. Films were scanned using a Cannon ImageRunner 3235 scanner. Band intensity was calculated using ImageJ (NIH Freeware).

E-cadherin, unique to cell plasma membranes, was used as a marker of reliable separation between membrane [M] and cytosolic [C] fractions. GAPDH or α-actinin were used as

protein loading controls for the cytosolic fraction, where appropriate. E-cadherin separations equivalent to membrane fractions >95% and cytosolic fractions <5% confirmed consistent subcellular fraction separation across all treatment groups (and vice versa for GAPDH where >95% was in the cytosolic fraction).

Ras Activation Assay

Cytoskeleton's Precision Red Advanced Protein Assay Reagent was used to determine total protein concentration in each of our samples. Ras GTPase activity was measured in the membrane and cytosolic fractions using the Ras Activity ELISA Assay Kit (EMD Millipore, Billerica, MA), which utilizes a recombinant Raf-1-RBD to bind active Ras. The assay was performed as per the manufacturer's instructions using 20 μg/μL total protein concentration. Active Ras was measured using the Packard LumiCount Luminometer Plate Reader, version 3.0, at λ=600 nm (Perkin Elmer, Waltham, MA).

BALF Cytokine and Chemokine Assay

Cytokine screening for selected helper T-cell type 1 (Th1) and helper T-cell type 2 (Th2) cytokines and chemokines from BALF supernatant was performed using MILLIPLEX MAP Mouse Cytokine/Chemokine Magnetic Bead Panel (Millipore, St. Charles, MO). The cytokine panel included IL-13, IL-4, IL-5, eotaxin, IL-10, IL-1α, IL-1β, IL-2, IP-10, IL-12, MCP-1, IL-9, VEGF, KC, G-CSF, LIX, MIP-1α, MIP-1β, MIG, LIF, M-CSF, RANTES, IL-17, IL-3, IL-7, IL-12, IL-15, GM-CSF, IFNγ, IL-6, MIP-2, and TNFα. For cytokine/chemokine sample measurements below the detection limit, results were assigned a value equal to the minimal detection limit for the specific assay to facilitate statistical analysis.

Histological Analyses

Paraffin-embedded left lung lobes were sectioned at 5 μm, parallel to the major conducting airways. Tissue sections were selected for staining by visual evaluation of airway branching to maximize the representation of conducting airways. Periodic Acid-Schiff (PAS) and hematoxylin & eosin (H&E) staining was performed on sections from 2 to 3 animals per group as described in Zeki *et al.* [7].

PAS stained sections were scored as follows: From each lung section, 5 regions were evaluated, consisting of 2 segments of primary conducting airway, 2 secondary conducting airways, and 1 tertiary conducting airway. A minimum of 100 sequential airway cells were counted from each region, and the total number of PAS-positive cells per total airway cells was determined. The regional values were averaged to give a final PAS score per animal termed "%PAS (+) Epithelial Cells" as seen in Figure 8.

H&E stained lung sections were scored by two treatment-blinded investigators. Peribronchial and perivascular inflammation were evaluated based upon a subjective scale of 0 to 5. Each slide was reviewed randomly and scored independently by at least two investigators. Scores were based on the following scale: 0 = no detectable inflammation, 2.5 = moderate inflammation with a layer of inflammatory cells encircling the bronchi and peribronchioles approximately three cells deep, and 5 = extensive inflammation with a layer

of inflammatory cells encircling bronchi and bronchioles greater than five cells deep. Scores were averaged for each animal denoting the “Inflammation Grade” as seen in Figure 6B.

Albumin Assay

The amount of albumin present in the supernatant of our BALF was measured using a Mouse Albumin ELISA kit (GenWay Biotech, Inc.). The BALF supernatant was diluted to a concentration of 1:80,000 using the diluent provided in the kit. The protocol provided in the kit was followed as per the manufacturer’s instructions. The assay was read using the Emax® Endpoint ELISA Microplate Reader from Molecular Devices, set at a wavelength of 450 nm. Data are represented as optical density (O.D.).

Cell Culture

HBE1 cells are an immortalized human bronchial epithelial cell line[31–35]. HBE1 cells (passage 18) were grown to at least 90% confluence on a 100 mm cell culture plate in serum-free medium containing Ham’s F12/DMEM (1:1), 15 mM $NaHCO_3$, 15 mM Hepes (pH 7.4), with the following six factors: transferrin (5 μg/mL), insulin (5 μg/mL), cholera toxin (10 ng/mL), epidermal growth factor (10 ng/mL), dexamethasone (0.1 μM), bovine hypothalamus extract (15 μg/mL), then transferred to 6-well plates under submerged media conditions. All treatments were performed in triplicate in at least three independent experiments to verify findings.

Experiment #1 (n=3)—For examination of FTI-277 effects on Ras translocation between cytosol and membrane. HBE1 cells grown to ≥ 90% confluence were treated with DMSO drug vehicle, 10 μM FTI-277 and 20 μM FTI-277 for 30 minutes. After FTI treatment, the medium was removed and adherent cells were homogenized and processed by ultra-centrifugation into cytosolic [C] and membrane [M] fractions.

Experiment #2 (n=3)—HBE1 cells grown to ≥ 90% confluence were pre-treated with FTI-277 (20 μM), FPP (10 μM), FTI+FPP, or vehicle control for 60 hours followed by 12-hour co-stimulation with IL13 (20 ng/mL) (total of 72-hours drug treatment duration). Additional experiments using lower FTI-277 doses at 5 and 10 μM were also conducted. Cell-free media were collected for eotaxin-3 ELISA measurements, and adherent cells were treated with RIPA buffer containing a Protease Inhibitor cocktail (1:100, Sigma-Aldrich), phenylmethanesulfonylfluoride (PMSF) (1 mM, Sigma-Aldrich) and Phosphatase Inhibitor (1:100, Sigma-Aldrich) for isolation of protein from cell homogenates. Media was ultra-centrifuged at 10,000 rpm at 4°C for 10 minutes, then cell-free culture medium supernatant was collected and stored at −80°C.

We used standard brightfield light microscopy and the Alamar blue assay to assess cell morphology, viability, and mitochondrial function. We did not detect any adverse or cytotoxic effect(s) of FTI-277, FPP, or their respective vehicles (DMSO or methanol:NH_4OH) alone or in combinations at the doses and treatment durations used in all of our experiments.

Epithelial Cell Tissue Homogenization and Fractionation

Cells from Experiment #1 were scraped and suspended in isolation buffer (250 mM sucrose, 20 mM HEPES, pH 7.4, 2 mM EDTA, and 3 mM NaN_3) containing protease inhibitors (Protease Inhibitor (1:100, Sigma), 1 mM PMSF, 1 mM Na_3VO_4, and 1 mM NaF) and Phosphatase Inhibitor (1:100, Sigma-Aldrich). Further homogenization was performed by hand using a pre-chilled dounce homogenizer. The resulting crude homogenates were centrifuged at 800 *g* for 5 min at 4°C. The supernatant was removed and reserved as "total" homogenate. An aliquot of this "total" homogenate was ultra-centrifuged again at 17,500 rpm (~30,000 *g*) at 4°C for an additional 30 minutes to separate the cytosolic and membrane components. The supernatant from this step was collected and referred to as the "cytosolic" fraction. The remaining pellet was re-suspended in the same volume of isolation buffer and considered as the "membrane" fraction.

Like our mouse specimens, proper subcellular fractionation was confirmed by assessing for a membrane-only constituent protein (E-cadherin), and a cytosol-only constituent protein (GAPDH). These proteins were used as a marker of reliable separation between membrane and cytosolic fractions. E-cadherin separation equivalent to membrane fraction >95% and cytosolic fraction <5% confirmed consistent and successful separation of subcellular fractions across all treatment groups.

The total protein concentration of the cytosolic fraction from each sample was measured using the Micro BCA Protein Assay Kit (Pierce Biotechnology, Rockford, Ill) and used to determine protein loading volumes for each sample.

Eotaxin-3 ELISA

Eotaxin-3 peptide concentration in HBE1 cell media was determined in the cell-free supernatant. Eotaxin-3 peptide concentrations (pg/mL) were determined using the DuoSet ELISA kit, performed according to the manufacturer's instructions (R&D Systems, Minneapolis, Minnesota) and per our standard ELISA lab techniques.

Statistical Analysis

Data were analyzed using the Prism 5 software package (GraphPad, Inc.; San Diego, CA). Raw data were assessed for normality using D'Agostino and Pearson omnibus test, and then tested for statistical significance using parametric or non-parametric tests, where appropriate. Values greater than 2 standard deviations (SD) outside the mean were not included in relevant analyses. Parametric data were analyzed using *t test*, 1-way ANOVA with Tukey post-test correction, or 2-way ANOVA with Bonferroni post-test correction. Non-parametric data were analyzed using the Mann-Whitney or Kruskal-Walis test with Dunn's post-test correction. Where necessary, some data were log transformed prior to statistical analysis. Data are plotted as means ± SEM except where indicated. A 2-tailed alpha was used in all analyses, and a p-value of <0.05 was considered statistically significant.

RESULTS

Blockade of Ras farnesylation through FTase inhibition with FTI-277 shifts subcellular localization of Ras from the membrane to the cytosol[36,37], and results in loss of Ras signaling activity (Figure 1). Therefore, we designed experiments using both mice and HBE1 human bronchial epithelial cells to measure Ras protein levels in the membrane and cytosol of mouse whole lung and cultured HBE1 cell homogenates. To assess FTI-277 effects on Ras GTPase function, we also measured Ras enzyme activity in those same subcellular fractions as Ras protein expression in mouse lungs, and correlated our findings to indices of inflammation, airway epithelial remodeling, and lung physiology.

We utilized FTI-277 in the same *in vivo* mouse model of allergic airway inflammation used in our previously published simvastatin experiments to compare the effects of FTI-277 on the same indicators of allergic airway inflammation. Mice were treated daily for fourteen days with i.p. injections of FTI-277 in combination with OVA aerosol or FA exposure to assess changes in Ras protein and enzymatic activity in mouse whole lung tissue, in addition to the classic hallmarks of asthma pathology.

Ras Subcellular Localization in Mouse Lungs

In FA mice, total Ras protein present in the membrane fraction was greater than Ras in the cytosolic fraction (Figure 2A). In contrast, mice exposed to OVA aerosol showed no significant difference in Ras protein levels between the membrane and cytosolic fractions indicating a relative increase in Ras cytosolic fraction relative to membrane fraction (Figure 2). In both exposure groups FA and OVA, treatment with FTI-277 had no significant effect on either total Ras protein expression (Figure 2B) or Ras cytosolic and membrane distribution in whole lung tissue homogenate (Figures 2A, 2C, 2D). In Figure 2A, all cytosolic bands represent unfarnesylated Ras including the faint band above the lowest one (dashed black arrow), and the membrane bands represent farnesylated membrane-anchored Ras (solid black arrows).

In the OVA groups in Figure 2D, we observed that there was a relative increase in the Ras cytosolic fraction relative to membrane fraction. It is not clear whether this is a result of membrane-to-cytosol Ras translocation or to an increase in cytosolic Ras due to the influx of inflammatory cells such as eosinophils. These data indicate that while OVA exposure alters the relative ratio of cytosolic to membrane-associated Ras, treatment with FTI-277 does not alter Ras translocation between cell membrane and cytosol in mouse whole lung homogenate at the dose and the time evaluated.

Ras GTPase Enzyme Activity in Mouse Lungs

In addition to assessing changes in subcellular localization of Ras protein, we also measured Ras GTPase enzymatic activity in both the unfractionated total homogenate and the cytoplasmic and membrane subcellular fractions.

In the *unfractionated* homogenates, when animals were combined by exposure type (OVA vs. FA) Ras GTPase activity in the OVA group was 2.61-fold higher than FA-exposed control mice (**p=0.0022 by *t test*, Figure 3A). Treatment with FTI-277 had no measureable

effect on total Ras GTPase activity in either the OVA or FA groups compared to their corresponding vehicle controls (Figure 3B). However, as compared to Figure 3A, OVA exposure resulted in higher Ras GTPase activity as compared to FA controls in the FTI-treated mice (Figure 3B, *p<0.05 by 1-way ANOVA). This indicates that OVA exposure is associated with increased Ras GTPase activity likely secondary to increased lung inflammation.

Using the *fractionated* samples, we compared Ras GTPase activity in the cytosolic and membrane fractionated lung samples. FA-exposed mice had significantly greater Ras GTPase activity in the membrane fraction as compared to the cytosolic fraction (***p<0.001 by 1-way ANOVA, Figure 3C), corresponding to Ras subcellular distribution in Figure 2A. OVA-exposed mice had no statistically significant differences in Ras GTPase activity between the two fractions (Figure 3C), also consistent with the Ras subcellular distribution shown in Figure 2D. The pattern of relative Ras protein expression in the different subcellular compartments (Figure 2D) appears to correlate with the pattern of Ras GTPase activity (Figure 3D), indicating that Ras enzyme activity likely reflects Ras protein levels *in vivo* in whole lung specimens. These data indicate that at baseline in naïve non-inflamed mice, Ras GTPase is predominantly membrane-bound (Figure 2) and enzymatically active (Figure 3). And under OVA-induced inflammation, Ras GTPase has increased enzymatic activity in both the cytosolic and membrane fractions; as compared to FA control mice (Figure 3C).

When samples are separated by exposure group and FTI treatment, only the FA+PBS group had a statistically significant difference in Ras GTPase activity between the cytosol and membrane fractions (Figure 3D). Treatment with FTI-277 had no statistically significant effect on Ras GTPase activity in either the OVA or FA groups (Figure 3D). In addition, there was a near equalization in Ras GTPase activity between the cytosolic and membrane fractions in both OVA treatment groups (Figure 3D). This means that during OVA-induced inflammation there is a significant amount of Ras GTPase activity in the cytosol, unlike their respective FA controls. This finding suggests that *cytosolic Ras* can be active under certain conditions of inflammation, contrary to current dogma.

We did not further investigate whether this increase in cytosolic Ras activity was due to a change in Ras translocation inside resident lung cells, or the effect of increased cytosolic Ras activity in influxed lung inflammatory cells. Ras GTPase activity has a strong positive linear correlation with BALF total cell count and BALF absolute eosinophil count (Figure 3E) suggesting the increase in Ras activity may be driven by airway/lung eosinophilia.

Allergic Airway Inflammation

The Ras GTPase/ERK pathway drives the IL5-dependent effects on cellular proliferation and survival[22,38], which may augment eosinophilic inflammation. Biochemically, this requires the proper functioning of FTase and access to the FPP substrate to catalyze the Ras farnesylation reaction. We therefore hypothesized that inhibition of FTase with FTI-277 would disrupt Ras signaling and attenuate allergic airway inflammation in OVA-exposed mice. We measured the effect of FTI-277 on OVA-induced allergic inflammation by

measuring BALF leukocyte counts and cytokine levels, goblet cell hyperplasia, and histopathologic peribronchiolar inflammation by semi-quantitative scoring.

In our model of OVA-induced allergic inflammation, the eosinophil is the predominant leukocyte typically representing 70–80% of the BALF total leukocyte counts. In OVA-exposed mice, there was a trend of increased BALF total live cell count with FTI-277 treatment, but this did not achieve statistical significance (p=NS by 1-way ANOVA). Measured another way using BALF total inflammatory cells/per 10 hpf, FTI-277 treatment of OVA-exposed mice increased inflammatory cell influx by 1.72-fold (*p<0.05, by 1-way ANOVA, Figure 4A). Thus, contrary to our hypothesis, in OVA-exposed mice, treatment with FTI-277 caused a significant increase in total inflammatory cells present in BALF (Figure 4A), with a 2.58-fold increase in eosinophil numbers as compared to the vehicle control group (*p<0.01 by 1-way ANOVA, Figure 4B). However, treatment of OVA mice with FTI-277 did not significantly affect BALF macrophage, lymphocyte, or neutrophil cell counts as compared to OVA+PBS controls (p=NS, data not shown).

The effect of FTI-277 treatment on BALF inflammatory cell numbers was supported by visual scoring of peribronchial and perivascular inflammation using H&E stained histopathological lung sections. There was a marked increase in perivascular and peribronchiolar inflammatory cell infiltrate in OVA mice treated with FTI-277 compared to OVA-exposed mice treated with drug vehicle. No significant changes in inflammation were observed in the FA controls (Figure 4C and 4D). The presence of significant eosinophilic infiltration with moderate, multifocal perivascular and peribronchiolar to interstitial lymphoplasmacytic infiltration, few neutrophils, and limited alveolar histiocytosis was confirmed by an independent veterinary pathologist at U.C. Davis.

Given that our mouse model manifests a strong Th2 allergic response with high IL13 production[6], we expected activation of STAT6 signaling in lung tissues. As predicted, mice exposed to OVA showed robust STAT6 phosphorylation relative to FA controls, which had no STAT6 phosphorylation (in homogenized whole lung tissue) (p<0.05, by 1-way ANOVA, Figure 4E). OVA mice treated with FTI-277 had a 1.55-fold increase in STAT6 phosphorylation as compared to OVA control, however, this did not reach statistical significance (p=0.05, by 1-way ANOVA, Figure 4E). FA-exposed mice treated with FTI-277 or drug vehicle control showed no significant difference in STAT6 phosphorylation. To assess both the downstream chemokine targets of the STAT6 transcription factor and upstream STAT6-inducing cytokines, we measured eotaxin (downstream), and IL-4 and IL-13 (upstream) secreted peptide levels in the BALF. Surprisingly, BALF eotaxin levels were not significantly increased with FTI-277 treatment in the OVA groups (p=NS by 1-way ANOVA, Figure 4F). Similarly, BALF IL-13 and IL-4 levels were not significantly increased with FTI-277 treatment in the OVA groups (p=NS by 1-way ANOVA, Figure 4F). These results suggest that the increase in eosinophilic inflammation observed with FTI-277 treatment in the OVA group may occur by a IL4/IL13/STAT6/eotaxin-independent mechanism.

BALF Cytokine Levels

We measured a total of 32 cytokines in BALF supernatant using a multiplex assay. Treatment with FTI-277 did not have a statistically significant effect on the levels of the following BALF cytokines/chemokines: IL-5, IL-10, IL-1α, IL-1β, IL-2, IP-10, IL-12, MCP-1, IL-9, VEGF, KC, G-CSF, LIX, MIP-1α, MIP-1β, MIG, LIF, M-CSF, RANTES, IL-17, IL-3, IL-7, IL-12, IL-15, GM-CSF, IFNγ (data not shown). There were no significant differences in any of the cytokines analyzed between FTI-277-treated and vehicle-treated mice in the FA groups. However, in OVA exposed mice, treatment with FTI-277 reduced IL-6 concentration by 67.4% (*p=0.0258), MIP-2 by 46.3% (*p=0.0356), and TNFα by 49.6% (*p=0.05), all analyzed by 1-way ANOVA (Figure 5). These three cytokine/chemokine data appear to contradict the other measurements of inflammation showing greater allergic inflammation with FTI-277 treatment.

Goblet Cell Hyperplasia

Airway epithelial remodeling, which includes goblet cell metaplasia, is a cardinal feature of allergic asthma in both animal models and human disease. We hypothesized that treatment with FTI-277 would reduce (+)PAS-staining of goblet cells in mice exposed to OVA. Using a semi-quantitative scoring method, we observed that FTI-277 increased goblet cell metaplasia/hyperplasia in the OVA group (*p=0.025 by *t test*, Figures 6A and 6B). Filtered air mice showed no significant change with FTI-277 or vehicle treatment (Figure 6B).

Lung Physiology

In a methacholine (MCh) dose-response aerosol challenge, OVA-exposed mice typically manifest heightened baseline respiratory system resistance (Rrs), decreased baseline dynamic compliance (Cdyn), and increased airway hyperreactivity (AHR) as indicated by increased airway resistance at any given dose of MCh relative to their respective FA controls. We hypothesized that treatment with FTI-277 would attenuate OVA-induced airways hyperresponsiveness and improve dynamic lung compliance.

Contrary to our hypothesis, treatment with FTI-277 in the OVA group caused a statistically significant increase in Rrs and AHR at all three MCh doses (Figure 7A), and a statistically significant decrease in Cdyn, but only at the highest MCh dose of 2 mg/mL, relative to their respective control group OVA+PBS (Figure 7B). There were no statistically significant changes due to FTI-277 treatment in the FA groups. There was no evidence of significant interaction between treatment group and MCh challenge dose for either Cdyn or Rrs analyses (p=NS by 2-way ANOVA).

Alveolar-Capillary Membrane Barrier Integrity

Due to both the unexpected pro-inflammatory effects of FTI-277 and the simultaneous yet paradoxical decrease in BALF cytokines (IL6, MIP-2, TNFα), we assessed whether this drug had any significant and direct pulmonary toxic effects independent of inflammation. We measured albumin levels in BALF supernatant as an indicator of alveolar-capillary membrane (ACM) barrier integrity because the loss of endothelial-alveolar barrier integrity would allow albumin to pass into the airspace, becoming detectible in lavage fluid.

Exposure to OVA greatly increased BALF albumin concentration relative to FA groups indicating a loss of ACM barrier integrity during allergic inflammation alone (Figure 8A and 8C). There was a statistically significant positive linear correlation between BALF albumin concentration and BALF total cell counts (Figure 8B), but treatment with FTI-277 did not significantly increase albumin levels between untreated controls and drug-treated mice for both OVA and FA groups (Figure 8C). This indicates that treatment with FTI-277 did not cause any significant direct injury to the ACM. Treatment with FTI-277, therefore, did not contribute to leukocyte leakage into the airspace or to inflammation by direct cytotoxic mechanisms.

Drug Tolerability

Treatment with FTI-277 did not hinder normal weight gain in mice in either the OVA- or FA-exposed groups. Average weights (±SEM) were as follows: OVA+PBS = 28.4±0.25, OVA+FTI = 28.2±0.06, FA+PBS = 28.0±0.23, FA+FTI = 28.2±0.23 (p=NS, by 1-way and 2-way ANOVA). Of note, weight alone as a single indicator of systemic toxicity is not a detailed enough measure to completely rule out subtle organ damage or other toxic drug effects, but weight gain is generally considered a reliable measure of good health and drug tolerability in experimental mice[39].

Ras Farnesylation in HBE1 Cells

To further investigate the effects of FTI-277 in a single-cell type without the more complex *in vivo* situation, we utilized the HBE1 cell line. We selected human bronchial epithelial cells given their central role in the pathogenesis of human asthma[40–42], and our established IL13 *in vitro* model of mucosal Th2 inflammation[11,43]. We first confirmed that, at pharmacologically relevant doses, FTI-277 inhibits FTase by measuring Ras translocation between cell plasma membrane and cytosol in ultra-centrifuged subcellular fractions.

Based on the knowledge that farnesylation is necessary for Ras GTPase membrane anchoring, we treated HBE1 cells with FTI-277 (10 or 20 μM for 30 minutes), or drug vehicle and determined the proportion of subcellular membrane ([M]) versus cytosolic ([C]) Ras (Figure 9). ‘Total’ Ras represents the sum of the membrane and cytosolic fractions, previously determined in separate exploratory experiments to be equivalent to the direct measurement of total Ras by Western blot of unfractionated total cell homogenates. Without FTI-277 treatment, Ras is predominantly present in the cell membrane (Figure 9A). Treatment with FTI-277 changed the ratio of membrane to cytosolic Ras in a dose-dependent manner showing greater cytosolic and lower membrane Ras, as expected (Figures 9A, 9C, 9D). Treatment with FTI-277 also increased the expression of total Ras (Figure 9B). The additional two bands seen above the lowest band in the Ras cytosolic fractions (Figure 9A, dashed black arrows) represent other unfarnesylated Ras proteins/isoforms[44], which also increase in a dose-dependent manner with FTI-277 treatment. By contrast, farnesylated Ras protein is membrane-bound (Figure 9A, solid black arrow). These data confirm the drug’s known mechanism of action at the FTI-277 doses utilized in our *in vitro* experiments, i.e. the inhibition of Ras farnesylation.

Effects of FPP and FTI-277 on Eotaxin-3 Secretion in HBE1 Epithelial Cells

IL13 is a major cytokine important in human asthma where IL13 antagonists are currently being studied as potential treatment for asthma[45]. IL13 is a potent inducer of eotaxin gene expression in endothelial and epithelial cells via the transcription factor STAT6[15,46–51]. The three human eotaxins (eotaxin-1 (CCL11), eotaxin-2 (CCL24), eotaxin-3 (CCL26)) are potent chemokines for the recruitment of eosinophils into the lung and airway tissues[50–55]. Of these three eotaxins, eotaxin-2 and eotaxin-3 are most relevant to human severe asthma where both are known to persist despite treatment with corticosteroids[27,55]. Eotaxin-3, in particular, has the best correlation with other biomarkers of Th2-high inflammation in human asthma[26,56,57]. We therefore, chose to study the IL13/STAT6/eotaxin-3 signaling axis in our HBE1 cell experiments given its clinical relevance.

We previously observed a decrease in eotaxin-3 secretion from HBE1 cells treated with the HMG-CoA reductase (HMGCR) inhibitor, simvastatin[11], and this statin inhibition occurred by a MA-dependent mechanism implicating FPP, GGPP, and/or cholesterol pathways (Figure 1). Given the potential role of FPP[58] and Ras in allergic asthma, and the results from our mouse experiments, we wanted to determine if FTI-dependent inhibition had a similar effect on IL13-induced eotaxin-3 secretion. To this end, HBE1 cells were pretreated with FTI-277 or FPP for 60 hours followed by stimulation with IL13 (+FTI-277 or +FPP) for the last 12 hours to induce eotaxin-3 production and extracellular peptide secretion (total of 72 hours exposure to FTI-277 (5, 10, and 20 μM) and/or FPP (10 μM)). Given the known IC_{50} of 50 nM, we expected that at the micromolar doses of FTI-277 used (and 72-hours treatment duration) all Ras GTPases would be fully inhibited. All IL13/STAT6/eotaxin-3 experiments were done at a FTI-277 treatment duration of 72 hours (Figure 10). Effects of FPP and FTI-277 on eotaxin-3, STAT6, and Ras subcellular localization were confirmed in multiple experiments. Measurements were made on the same cell samples for Ras and STAT6 and their respective cell-free media for eotaxin-3 ELISA.

Unlike Figure 9A where the unfarnesylated Ras proteins were visualized as multiple bands in the cytosolic [C] fraction (dashed black arrows), in Figures 10D and 10E, only one band is seen in the [C] fraction which represents unfarnesylated Ras. The key difference between the experiments represented by Figures 9 and 10 is the time-point of 30 minutes versus 72 hours, respectively.

In un-stimulated/control HBE1 cells, treatment with FTI-277 or FPP had no effect on basal secretion of eotaxin-3 (Figure 10A). As expected, IL13 stimulation of HBE1 cells increased eotaxin-3 secretion by 11.3-fold compared to unstimulated control cells. In contrast to the effects of simvastatin[6,11], treatment of HBE1 cells with FTI-277 had no significant effect on IL13-induced eotaxin-3 peptide secretion (Figure 10A) or STAT6 phosphorylation (Figure 10B). This is consistent with the lack of inhibition of eotaxin-3 secretion since STAT6 controls eotaxin-3 gene expression. However, exogenous treatment of IL13-stimulated cells with the MA metabolite FPP *unexpectedly and significantly* increased STAT6 phosphorylation by 1.53-fold (*$p<0.05$ by 1-way ANOVA; Figure 10C) and augmented eotaxin-3 secretion by 3.2-fold compared to IL13 alone (*$p<0.001$ by 1-way ANOVA, Figure 10A). As the graph shows, this is consistent with a *synergistic* effect of combined IL13+FPP on eotaxin-3 secretion as compared to IL13 and FPP separately.

Given the effects of FPP on IL13-induced eotaxin-3 secretion and lack of eotaxin-3 inhibition by FTI-277, we evaluated the role of Ras subcellular localization, i.e. farnesylation, at this 72-hour time-point. For control groups, the majority of Ras was located in the cytosolic fraction (Figures 10D and 10E, *$p<0.05$ by 2-way ANOVA), unlike at the 30-minute time-point where the majority of Ras was in the membrane (Figure 9A). Treatment with FPP, IL13, or IL13+FPP was associated with translocation of Ras from the cytosol to the membrane as compared to the control group (Figure 10D, $^{f,\Phi}p=0.0043$ by 1-way ANOVA comparing cytosolic or membrane fractions across treatment groups; **$p<0.0001$ by 2-way ANOVA comparing C vs. M fractions for each treatment group). However, there were no significant differences between the IL13 and IL13+FPP groups with respect to the cellular localization of Ras. This suggests that the FPP-augmented IL13-induced STAT6 phosphorylation (Figure 10C) and eotaxin-3 secretion (Figure 10A) occurs by a mechanism independent of changes in Ras farnesylation.

With respect to treatment with FTI-277, this caused an unexpected and paradoxical increase in the membrane fraction as compared to cytosol at this 72-hour time-point (Figure 10E, **$p<0.01$ by 2-way ANOVA). Based on the known mechanism of action of FTI-277 (Figure 1), we had expected an increase in the cytosolic fraction and a decrease in the membrane fraction of Ras, as we saw in Figure 9. Treatment with IL13 induced translocation of Ras from the cytosol to the membrane as compared to the control group (Figure 10E, $^{f,\Phi}p=0.0385$ by 1-way ANOVA comparing cytosolic or membrane fractions between treatment groups for IL13 only; **$p<0.01$ by 2-way ANOVA comparing C vs. M fractions for the IL13 and FTI treatment groups). Like the FPP experiment above, there were no statistically significant differences between the IL13 and IL13+FTI groups with respect to the cellular localization of Ras. This confirms that at the 72-hour time point, treatment with FTI-277 failed to significantly affect the subcellular location of Ras in the expected manner (i.e. increase cytosolic Ras and decrease membrane Ras), unlike at the 30-minute time point which did inhibit Ras farnesylation, and thereby, depleted Ras from cell membranes while enriching cytosolic Ras (Figure 9).

These are key findings because pharmacologic inhibition of FTase does the following: 1) blocks Ras farnesylation, and therefore, inhibits Ras membrane enrichment (Figure 1) and subsequent kinase-mediated signal transduction, and 2) blocks the utilization of FPP thereby increasing local intracellular FPP concentrations. There are several important implications of these two effects which we address in the Discussion, where we also explore potential alternative interpretations of these data.

DISCUSSION

We sought to determine whether pharmacological inhibition of farnesyltransferase (FTase) with FTI-277, a potent Ras CaaX domain peptidomimetic, attenuates ovalbumin-induced allergic inflammation, epithelial remodeling, and AHR, as well as, reduce Ras GTPase activity. This is the only study we are aware of that systematically assesses the therapeutic potential of FTase inhibition in a murine model of asthma, and in an *in vitro* model of epithelial type-2 immune activation using human bronchial epithelial cells.

Our hypothesis derives from our understanding of the biochemistry of the MA pathway and its two basic arms, the non-sterol (i.e. isoprenoid) and sterol (i.e. squalene, cholesterol) arms (Figure 1). Increasingly, there is greater appreciation that the MA pathway plays a critical role in adaptive immune responses, T-cell polarity and proliferation, and Th2-mediated allergic inflammation[6,59,60].

Given that HMGCR inhibitors (e.g. statins) and GGTase inhibitors have been previously shown to mitigate allergen-induced airway inflammation in animal models[6,16,18,24,25,61], and given the Th2 pro-inflammatory role of Ras in eosinophil biology and allergic inflammation[19,21,23], we reasoned that inhibiting FTase activity would indirectly inhibit Ras GTPase signaling by blocking Ras farnesylation (Figure 1). Without this farnesyl tail, Ras cannot anchor in cell membranes rendering it functionally inactive, thus, inhibiting Ras-mediated downstream signal transduction[62–64]. Therefore, our hypothesis predicted that FTase inhibition would inhibit Ras-mediated allergic eosinophilic inflammation and the development of experimental asthma.

Our main findings can be summarized as follows: In naïve non-inflamed mouse lungs Ras protein is located predominantly in cell membranes (Figures 2), where it is enzymatically active (Figure 3). This indicates that Ras is constitutively active *in vivo* and participates in normal homeostatic respiratory cellular physiology. Contrary to our hypothesis, inhibition of Ras farnesylation via pharmacologic antagonism of FTase using FTI-277 further exacerbates allergic airway inflammation (Figure 4) and goblet cell hyperplasia (Figure 6), and worsens AHR (Figure 7). Therefore, pharmacologic disruption of FTase activity and Ras farnesylation may be harmful as a therapeutic strategy in asthma. Our results contradict previous work by other investigators who showed that Ras is a critical player in establishing the Th2 response in asthma[19,21]. In IL13-stimulated HBE1 cells, FTase inhibition with FTI-277 did not affect Ras membrane and cytosol levels, IL13/STAT6 signaling, or eotaxin-3 peptide secretion. However, the addition of exogenous FPP to these cells synergistically increased IL13-induced STAT6 phosphorylation and eotaxin-3 peptide secretion (Figure 10A–C), and this FPP effect occurs independent of Ras farnesylation (Figure 10D). In summary, these data indicate that lung Ras GTPase is important in normal physiological function, inhibition of Ras farnesylation *in vivo* promotes Th2 inflammation and asthma pathogenesis, and excess FPP augments the pro-inflammatory effects of IL13 on eotaxin-3 peptide secretion from airway epithelial cells. Our results highlight the complex role of the MA cascade in allergic inflammation relevant to human asthma, and further suggest that rather than antagonizing FTase, depletion of FFP in the airways might confer therapeutic benefits in asthma (Figure 11).

In support of this idea, inhibition of the enzyme farnesylpyrophosphate (or diphosphate) synthase (FPPS) by the bisphosphonate (BP) drug alendronate, attenuates eosinophilic airway inflammation and suppresses eotaxin-2 production in lung macrophages[65]. Being a key enzyme in the MA pathway, FPPS synthesizes FPP (Figure 1), therefore, alendronate acts similarly to statins in that both drugs reduce the pool of available FPP inside cells. Conversely, treatment with FTI-277 may increase the pool of available FPP[66] which can then be shunted to GGPP (Figures 1 and 11B). This in turn can increase geranylgeranylation of Rho, Ras, and/or Rab GTPases and lead to increased cell signaling, proliferation, cell

migration, vesicle trafficking/release, and inflammation[67–71]. Thus, we speculate that diversion of FPP to other metabolites in the MA cascade is possible (Figure 11B and 11C), among other potential mechanisms. Thus, FPP-enhanced IL13/STAT6 signaling in airway epithelial cells may be a novel therapeutic target independent of Ras, worthy of further study.

Mevalonate- and FTase-Dependent Immune Modulation

The MA pathway contributes to and regulates T-cell mediated immune responses, in particular antigen presenting cells, dendritic cells, T-cell activation[72,73], and Th1/Th2 polarity[13,59,60]. We previously showed that MA mediates Th2 allergic inflammation and lung eosinophilia in our mouse model[6]. Simvastatin also inhibits T-cell activation by impairing the function of Ras superfamily small GTPases like Ras, Rac, and Rab GTPase, key proteins activated by the isoprenoids FPP and GGPP[74] in the MA pathway (Figure 1). Statins also negate Th2 allergic responses by reducing T-cell activity/proliferation and IL4/IL13 cytokine production[4,6,75].

In our current study, however, while FTI-277 treatment did not significantly affect mouse BALF IL4, IL13, IL5, or eotaxin levels, we did see significant amplification of eosinophilic inflammatory cell recruitment to the lung and increased airway remodeling as defined by goblet cell metaplasia/hyperplasia. Conversely, treatment with the FTI-277 reduced BALF levels of IL6, MIP-2, and TNFα (Figure 5) despite the simultaneous increase in eosinophilic inflammation. Similarly, Xue *et al.* noted a significant down regulation of Th1 cytokine secretion with the FTase inhibitor, tipifarnib, including reductions in IL6, IL1β, and TNFα, like we observed in our experiments[76]. We speculate that by inhibiting Th1 polarity, FTI-277 indirectly enhanced Th2 responses resulting in worsening eosinophilic inflammation. Another possible explanation is the temporal relationship between cytokines and infiltrating inflammatory cells which may not be synchronized when we observe a single time point. Also, the pro-inflammatory effects of FTI-277 may not be occurring primarily via enhanced cytokine induction.

In our *in vitro* epithelial cell model, we chose to study IL13-induced eotaxin-3 production as an indicator of type 2 inflammatory mucosal immune responses relevant to human asthma. The eotaxins (eotaxin-1 (CCL11), eotaxin-2 (CCL24), and eotaxin-3 (CCL26)) are well-characterized potent chemoattractants for systemic and tissue eosinophilia. While FTI-277 treatment led to no significant changes in IL13-induced STAT6 phosphorylation or eotaxin-3 secretion in HBE1 cells, the addition of exogenous FPP to HBE1 cells caused a significant increase in IL13-induced STAT6 phosphorylation and eotaxin-3 secretion, and this occurred independent of Ras farnesylation (Figure 10D). If farnesylation is playing an important role in this mechanism, then this suggests that farnesylation of a protein (or proteins) other than Ras (Figure 11A) may be involved. Thus, Ras-*independent* protein farnesylation versus other direct FPP effects might be a novel mechanism and undiscovered part of the IL13/STAT6/eotaxin signaling axis in airway epithelial cells (Figure 11B–D).

Ras, FTase, and the Role of FTI-277 Treatment in Allergic Asthma

The Ras subfamily is a major intracellular signaling hub and functions to regulate many basic cellular processes. This includes signal transduction pathways involved in cellular proliferation, differentiation, polarization, cell growth, and cell motility important in cell biology, health, and diseas[2,12,13,36,66,77–82], in addition to the fundamental role that Ras plays in many cancers[2,83–88]. The FTase enzyme recognizes the CaaX box motif on the C-terminus of Ras, covalently binds a farnesyl group to the terminal cysteine residue, and releases its pyrophosphate (PP) group[13]. FTI-277 is a potent Ras CaaX domain peptidomimetic that competes with Ras for the FTase active site[89] (Figure 1).

Ras, FPP, and protein farnesylation have been examined to a limited degree in asthma[19,65]. Ras plays a role in IL5-induced eosinophil transmigration when examined *in vitro*[90]. Experiments using a dominant negative HIV-TAT Ras construct showed that Ras was necessary for the induction of the Th2 allergic response in mice[19].

In our study, treatment with FTI-277 *in vivo* had no significant effects on Ras cytosolic and membrane subcellular distribution in either FA or OVA exposure groups, or on total Ras protein expression in whole lung tissue homogenate (Figure 2). Similarly, Ras GTPase activity was also not affected by drug treatment (Figure 3). Despite these findings, treatment with FTI-277 exacerbated allergic inflammation (Figure 4) and worsened lung function in mice (Figure 7) indicating that it did have a significant yet negative pharmacologic effect in our mouse model.

The FTI-277 dose administered in mice was sufficiently high enough to inhibit FTase and subsequent Ras farnesylation. Based on our dosing regimen (see **Methods**), mice received the equivalent of 6.3 mM of FTI-277 per day, which is not only six orders of magnitude higher than the drug's IC_{50} of 50 nM, but is three orders of magnitude higher than the drug concentrations used in our cell culture experiments (10 and 20 μM, Figure 10). Therefore, either measuring Ras (and its GTPase activity) in whole lung homogenate does not provide enough detail or granularity to detect such small changes in signaling, or the adverse effect of FTI-277 treatment in our model occurs by a different mechanism.

Effects of FPP and FTI-277 Treatment in HBE1 Cells

Using HBE1 cells *in vitro*, FPP augmented IL13-induced STAT6 activation and eotaxin-3 secretion (Figure 10A and 10C), but the lack of any significant differences in Ras cytosol and membrane content between IL13 and IL13+FPP (Figure 10D) suggests a Ras-independent mechanism (Figure 11). While it is reasonable to think that the observed FPP effect likely involves Ras-independent farnesylation of proteins that then promote IL13/STAT6 signaling (Figure 11A), there may be other important effects of FPP not yet elucidated in bronchial epithelial cells involving Rab GTPase, cholesterol, or phosphoantigen signaling (Figure 11B–D).

There are several plausible explanations for the lack of significant differences in Ras farnesylation between the IL13 vs. IL13+FTI groups. One possibility is insufficient FTI-277 inhibition of FTase which is tantamount to no inhibition of Ras farnesylation. However, this is highly unlikely given the high treatment concentrations used (10 and 20 μM) relative to

the known IC_{50} of the drug (50 nM). We confirmed pharmacologic inhibition of Ras farnesylation by showing that FTI-277 significantly decreased the ratio of membrane-bound Ras while increasing cytosolic unprenylated Ras in epithelial cells (Figures 1 and 9).

However, treatment durations over a 72-hour timeframe or longer (as in our mouse experiments), could lead to an *increase* in the intracellular pool of available FPP, which when metabolized to GGPP (Figure 1), can lead to Ras geranylgeranylation[91]. This would in turn result in increased membrane-anchoring of geranylgeranylated Ras and increased Ras activation despite FTI-277 treatment. Biochemically-speaking, it is possible that as the levels of farnesylated Ras declined due to FTI-277 treatment, geranylgeranylated Ras increased to yield a net of no significant change in membrane and cytosolic Ras (Figure 10E). This mechanism could also explain the paradoxical enrichment of Ras membrane-anchoring post FTI-227 treatment (Con. versus FTI, Figure 10E). Whereas at shorter FTI-277 treatment durations (i.e. 30 minutes, Figure 9A), this potential alternative geranylgeranylation does not seem to occur.

There are at least four other explanations for the lack of FTI-277 treatment effect. First, despite the fact that FTI-277 doses used in all of our animal and cell culture experiments far exceeded the drug's IC_{50} for FTase, it is possible that FTase inhibition of Ras farnesylation was not sufficient to block signaling of all three Ras isoforms (K-, H-, and N-Ras)[14,79,92,93] resulting in residual Ras membrane tethering and continued Ras activity. Second, in addition to the known Ras post-translational modifications of farnesylation and geranylgeranylation that facilitate membrane anchoring, Ras can also undergo palmitoylation[94]. Our experiments did not assess for palmitoylation, therefore, this could also potentially explain persistent Ras activation despite FTase inhibition with FTI-277. Third, Ras GTPase can also undergo phosphorylation by kinases which also controls its activity[80]. And fourth, having confirmed the FTI-277 dose range (10 to 20 μM, Figure 9A) that inhibits FTase at the shorter 30-minute time-point, we speculate that it is possible that the drug was metabolized or compensatory mechanisms became active by 72 hours such that FTase was no longer effectively inhibited.

The Diverse Roles and Effects of FPP

FPP plays important roles in cellular biochemistry and physiology, and airway function is no exception. FPP is utilized both for farnesylation, which is necessary for the incorporation of small GTPases such as Ras into cell membranes, and as the precursor molecule for GGPP and cholesterol. In an *ex vivo* model of asthma, the addition of FPP or GGPP enhanced LPS-induced bronchoconstriction of isolated human bronchi[58], a mechanism relevant to human asthma pathogenesis.

Our results show that FPP exacerbates mucosal IL13-mediated chemokine production in line with type 2 inflammatory responses in the airways. This is an important and novel observation that will require further study. There are several potential explanations for the synergistic effect of IL13+FPP on eotaxin-3 peptide secretion (Figure 10A). The isoprenoid FPP has diverse biological roles in different disease models. In addition to its well-known role in Ras and protein farnesylation[13,64], FPP can be metabolized into different effector molecules and also has direct effects on cells. In the MA pathway, which is fundamentally

an anabolic cascade, FPP is metabolized to GGPP and further downstream to squalene then cholesterol (Figure 1) both of which can activate immune cells leading to inflammation[59]. These are critical molecules not only for the formation of cell membranes via cholesterol and small GTPase function for signal transduction, but also oxysterol metabolism and the regulation of various transcription factors important in lipid biology and inflammation[95,96] including the glucocorticoid receptor (GR)[97,66,82].

Like squalene synthase inhibitors (Figure 1), the FTIs can theoretically increase inflammation by increasing the pool of unused endogenous FPP which can farnesylate and activate GTPases in excess[66]. FPP itself could lead to increased farnesylation of other non-Ras small GTPases[79,98] (such as Rho family GTPases like RhoB [99–101]), farnesylation of non-GTPase proteins or kinases[81], and shunting of FPP to GGPP resulting in increased geranylgeranylation of Rho and/or Rab family GTPases (Figure 11B). For example, the antibiotic and FTase inhibitor manumycin competes with FPP as a substrate for the FTase enzyme. In doing so, it increases FPP concentrations locally and this can activate various transcription factors important in cell proliferation and inflammation[97].

In support of this idea, when we added FPP to IL13, we observed enhanced STAT6 phosphorylation in HBE1 cells (Figure 10C). While we have not investigated the mechanism underlying this novel observation, it may involve farnesylation of a protein (or group of proteins) involved in the IL13/STAT6/eotaxin cascade and/or due to direct FPP effects on epithelial cells. Figure 11 summarizes some hypothetical mechanisms that we propose involving FPP and potential cellular responses relevant to airway epithelial type 2 inflammation.

Phosphoantigen Biology and Asthma

Isopentenyl pyrophosphate (IPP), an isoprenoid metabolite just upstream of FPP (Figure 1), is the originally described “phosphoantigen”[102–104]. Extracellular IPP is detected by γδ–T-cells via the butyrophilin receptor family as part of their immune surveillance program against infection[103] and malignant transformation[105–110].

Relevant to our work, γδ–T-cells have also been recognized to play a role in asthma pathogenesis[111]. Given our results, is it possible that FPP could also function as a *phosphoantigen* (Figure 11D)? At least with respect to activating γδ–T-cells, there is evidence to suggest that FPP (and GGPP) may function as phosphoantigens or have phosphoantigen-like properties, but may be less potent than IPP[112]. Whether this also happens in airway epithelial cells remains unknown.

It is intriguing to speculate whether phosphoantigens also play a role in asthma as a ‘danger signal’ released by dying or diseased epithelial (or other types of) cells (Figure 11D). This may be an important mechanism to study if FPP causes a significant elevation in the intensity of Th2 inflammation in human asthma, specifically IL13-mediated signaling in the intact epithelial compartment. In a more general sense, *phosphoantigen biology* could be an important area to explore in the pathogenesis of asthma and other pulmonary diseases. Functionally-speaking, FPP also leads to bronchoconstriction in isolated human airways[58], a response relevant to asthma and lung physiology. The therapeutic implications of this idea

would be the development of novel therapies such as butyrophilin receptor antagonists or inhaled statins[113–116] and/or inhaled BPs[65], both of which deplete the pool of available FPP and GGPP, thus reducing the burden of isoprenoid phosphoantigens in the airways.

Conclusions

Our prior work collectively indicates that depletion of MA pathway metabolites may be a useful therapeutic strategy in asthma and allergic inflammation. This current study suggests that Ras farnesylation may not underlie the previously reported beneficial statin effects in asthma. Further, we have now shown that inhibition of FTase in allergic asthma *in vivo*, which specifically inhibits Ras farnesylation, may be harmful. However, Ras-independent protein farnesylation or direct cellular effects of FPP may contribute to airway epithelial Th2 cytokine production.

Beyond the statins alone, further research should continue to investigate the modulation of airway isoprenylation and the role of FPP in asthma pathogenesis. Based on our prior statin work, the results of this study, and recent publications assessing the role of FPPS, a therapeutic approach utilizing FPPS inhibitors (such as BPs) and/or HMGCR inhibitors (such as statins) might yield better results. Therefore, inhibition of the production or release of cellular FPP might be a better therapeutic strategy than FTase or Ras inhibition in asthma.

Acknowledgments

Grant/Funding Support: NIH T32 HL07013 (JMB, AAZ), NCATS UL1 TR000002 (AAZ), HL105573 (NJK), NCHCS VA Medical Center, and American Thoracic Society (ATS) Fellows Career Development Award (AAZ), KL2 RR 024144 (AAZ), 1K08HL114882-01A1 (AAZ), NIH-RO1- HL-66189 (TG), TRDRP-0087 (SF), NIOSH U54 OH007550 (JAL).

We would like to thank Keisha Williams, Simon Vu, and Kenneth Chmiel for their technical assistance and input.

Abbreviations

FTase	Farnesyltransferase
FTI	FTase inhibitor
PMSF	phenylmethanesulfonylfluoride
AHR	airway hyperreactivity
GGTase	geranylgeranyltransferase
FTI	farnesyltransferase inhibitor
HMGCR	3-hydroxy-3-methyl-glutaryl-CoA reductase
FTI-277	farnesyltransferase inhibitor-277
FPP	farnesylpyrophosphate
GGPP	geranylgeranylpyrophosphate
IPP	isopentenyl pyrophosphate

GTPase	guanosine triphosphatase
MA	mevalonate
OVA	ovalbumin
FA	filtered air
HBE1	human bronchial epithelial-1
STAT6	Signal transducer and activator of transcription 6
IL13	interleukin-13
ICS	inhaled corticosteroids
FPPS	farnesylpyrophosphate synthase
GGPPS	geranylgeranylpyrophosphate synthase
BALF	bronchoalveolar lavage fluid
DMSO	dimethyl sulfoxide
PVDF	polyvinylidene difluoride
PAS	Periodic Acid-Schiff
MCh	methacholine
FeNO	fraction of exhaled nitric oxide
ppb	parts per billion
Rrs	respiratory system resistance
Cdyn	dynamic compliance
ACM	alveolar-capillary membrane
BP	bisphosphonate
GDP	guanosine diphosphate
GTP	guanosine triphosphate
EGFR	epithelial growth factor receptor
GR	glucocorticoid receptor
hpf	high-power field

References

1. World Health Organization (WHO). Global Surveillance, Prevention, and Control of Chronic Respiratory Diseases: A Comprehensive Approach. 2007. p. 1-129.

2. Yeganeh B, Wiechec E, Ande SR, Sharma P, Moghadem AR, Post M, Freed DH, Hashemi M, Shojaei S, Zeki AA, Ghavami S. Targeting the mevalonate cascade as a new therapeutic approach in heart disease, cancer and pulmonary disease. Pharmacology & Therapeutics. 2014; 143(1):87–110. [PubMed: 24582968]

3. Chiba Y, Sato S, Misawa M. Inhibition of antigen-induced bronchial smooth muscle hyperresponsiveness by lovastatin in mice. J of Smooth Muscle Res. 2008; 44(3–4):123–128. [PubMed: 18832788]

4. Huang C-F, Peng H-J, Wu C-C, Lo W-T, Shih Y-L, Wu T-C. Effect of oral administration with pravastatin and atorvastatin on airway hyperresponsiveness and allergic reactions in asthmatic mice. Annals of Allergy, Asthma & Immunology. 2013; 110(1):11–17.

5. Ahmad T, Mabalirajan U, Sharma A, et al. Simvastatin improves epithelial dysfunction and airway hyperresponsiveness: from asymmetric dimethyl-arginine to asthma. American Journal of Respiratory Cell and Molecular Biology. 2011; 44(4):531–539. [PubMed: 20558777]

6. Zeki AA, Franzi L, Last J, Kenyon NJ. Simvastatin inhibits airway hyperreactivity: implications for the mevalonate pathway and beyond. American Journal of Respiratory and Critical Care Medicine. 2009; 180(8):731–740. [PubMed: 19608720]

7. Zeki AA, Bratt JM, Rabowsky M, Last JA, Kenyon NJ. Simvastatin inhibits goblet cell hyperplasia and lung arginase in a mouse model of allergic asthma: a novel treatment for airway remodeling? Translational Research. 2010; 156(6):335–349. [PubMed: 21078495]

8. Liao JK, Laufs U. Pleiotropic Effects of Statins. Annual Reviews of Pharmacology and Toxicology. 2009; 45(8):89–118.

9. Wang C-Y, Liu P-Y, Liao JK. Pleiotropic effects of statin therapy: molecular mechanisms and clinical results. Trends in Molecular Medicine. 2008; 14(1):37–44. [PubMed: 18068482]

10. Roy A, Jana M, Kundu M, et al. HMG-CoA Reductase Inhibitors Bind to PPARalpha; to Upregulate Neurotrophin Expression in the Brain and Improve Memory in Mice. Cell Metabolism. 2015; 22:253–265. [PubMed: 26118928]

11. Sandhu K, Ott S, Wu R, Zeki A. The Mevalonate Pathway Regulates Eotaxin-3 Secretion from Human Airway Epithelial Cells: A Therapeutic Role for Simvastatin in Asthma. Journal of Investigative Medicine. 2014; 62(1) Abstract #381.

12. McTaggart SJ. Isoprenylated proteins. Cellular and Molecular Life Sciences. 2006; 63(3):255–267. [PubMed: 16378247]

13. Greenwood J, Steinman L, Zamvil SS. Statin therapy and autoimmune disease: from protein prenylation to immunomodulation. Nat Rev Immunol. 2006; 6(5):358–370. [PubMed: 16639429]

14. Schmick M, Kraemer A, Bastiaens PI. Ras moves to stay in place. Trends in Cell Biology. 2015; 25(4):190–197. [PubMed: 25759176]

15. Goto K, Chiba Y, Matsusue K, et al. The proximal STAT6 and NF-kappaB sites are responsible for IL-13- and TNF-alpha-induced RhoA transcriptions in human bronchial smooth muscle cells. Pharmacological Research. 2010; 61(5):466–472. [PubMed: 20006706]

16. Chiba Y, Arima J, Sakai H, Misawa M. Lovastatin inhibits bronchial hyperresponsiveness by reducing RhoA signaling in rat allergic asthma. Am J Physiol Lung Cell Mol Physiol. 2008; 294(4):L705–L713. [PubMed: 18296496]

17. Schaafsma D, Roscioni SS, Meurs H, Schmidt M. Monomeric G-proteins as signal transducers in airway physiology and pathophysiology. Cell Signal. 2008; 20(10):1705–1714. [PubMed: 18538541]

18. Chiba Y, Sato S, Misawa M. GGTI-2133, an inhibitor of geranylgeranyltransferase, inhibits infiltration of inflammatory cells into airways in mouse experimental asthma. Int J Immunopathol Pharmacol. 2009; 22(4):929–935. [PubMed: 20074456]

19. Myou S, Zhu X, Myo S, Boetticher E, Meliton AY, Liu J, Munoz NM, Leff AR. Blockade of airway inflammation and hyperresponsiveness by HIV-TAT-dominant negative Ras. Journal of Immunology. 2003; 171(8):4379–4384.

20. Luo F. Simvastatin induces eosinophil apoptosis in vitro. Chest. 2004; 126(4):721S.

21. Hall DJ, Cui J, Bates ME, et al. Plenary paper Transduction of a dominant-negative H-Ras into human eosinophils attenuates extracellular signal – regulated kinase activation and interleukin-5–mediated cell viability. Blood. 2001; 98(7):2014–2021. [PubMed: 11567984]

22. Zhu Y, Bertics PJ. Chemoattractant-induced signaling via the Ras-ERK and PI3K-Akt networks, along with leukotriene C4 release, is dependent on the tyrosine kinase Lyn in IL-5- and IL-3-primed human blood eosinophils. Journal of Immunology. 2011; 186(1):516–526.
23. Shibata Y, Kamata T, Kimura M, Yamashita M, Wang CR, Murata K, Miyazaki M, Taniguchi M, Watanabe N, Nakayama T. Ras activation in T cells determines the development of antigen-induced airway hyperresponsiveness and eosinophilic inflammation. Journal of Immunology. 2002; 169(4):2134–2140.
24. McKay A, Leung BP, McInnes IB, Thomson NC, Liew FY. A Novel Anti-Inflammatory Role of Simvastatin in a Murine Model of Allergic Asthma. The Journal of Immunology. 2004; 172(5): 2903–2908. [PubMed: 14978092]
25. Kim D, Lim J, Lee Y, Ro J, Ryu S. Anti-inflammatory mechanism of simvastatin in mouse allergic asthma model. European Journal of Pharmacology. 2007; 557:76–86. [PubMed: 17169357]
26. Choy DF, Modrek B, Abbas AR, et al. Gene expression patterns of Th2 inflammation and intercellular communication in asthmatic airways. Journal of Immunology. 2011; 186(3):1861–1869.
27. Coleman JM, Naik C, Holguin F, et al. Epithelial eotaxin-2 and eotaxin-3 expression: relation to asthma severity, luminal eosinophilia and age at onset. Thorax. 2012; 67(12):1061–1066. [PubMed: 23015684]
28. Kenyon NJ, Gohil K, Last JA. Susceptibility to ovalbumin-induced airway inflammation and fibrosis in inducible nitric oxide synthetase-deficient mice: mechanisms and consequences. Toxicology and Applied Pharmacology. 2003; 191(1):2–11. [PubMed: 12915099]
29. Kenyon N, Ward R, Last J. Airway fibrosis in a mouse model of airway inflammation. Toxicology and Applied Pharmacology. 2003; 186:90–100. [PubMed: 12639500]
30. Kenyon NJ, Last JA. Reversible and irreversible airway inflammation and fibrosis in mice exposed to inhaled ovalbumin. Inflamm Res. 2005; 54:57–65. [PubMed: 15750712]
31. Robinson CB, Wu R. Culture of Conducting Airway Epithelial in Serum-Free Medium. J Tiss Cult Meth. 1991; 13(20):95–102.
32. Wu R, Nolan E, Turner C. Expression of tracheal differentiated functions in serum-free hormone-supplemented medium. J Cell Physiol. 1985; 125(2):167–181. [PubMed: 4055904]
33. Whitcutt MJ, Adler KB, Wu R. A biphasic chamber system for maintaining polarity of differentiation of culture respiratory tract epithelial cells. In Vitro Cellular and Developmental Biology. 1988; 24(5):420–428. [PubMed: 3372447]
34. Statt S, Ruan J-W, Hung L-Y, et al. Statin-Conferred Enhanced Cellular Resistance against Bacterial Pore-Forming Toxins in Airway Epithelial Cells. American Journal of Respiratory Cell and Molecular Biology. 2015; 53(5):689–702. [PubMed: 25874372]
35. Yankaskas JR, Haizlip JE, Conrad M, et al. Papilloma virus immortalized tracheal epithelial retain a well-differentiated phenotype cells. American Journal of Physiology. 1993; 264:C1219–C1230. [PubMed: 7684560]
36. Gibbs JB, Graham SL, Hartman GD, Koblan KS, Kohl NE, Omer CA, Oliff AA. Farnesyltransferase inhibitors versus Ras inhibitors. Current Opinion in Chemical Biology. 1997; 1:197–203. [PubMed: 9667853]
37. Efuet ET, Keyomarsi K. Farnesyl and geranylgeranyl transferase inhibitors induce G1 arrest by targeting the proteasome. Cancer Research. 2006; 66(2):1040–1051. [PubMed: 16424040]
38. So E-Y, Oh J, Jang J-Y, Kim J-H, Lee C-E. Ras/Erk pathway positively regulates Jak1/STAT6 activity and IL-4 gene expression in Jurkat T cells. Molecular Immunology. 2007; 44(13):3416–3426. [PubMed: 17433443]
39. Hesterberg TW, Gerriets JE, Reiser KM, Jackson AC, Cross CE, Last JA. Bleomycin-Induced Pulmonary Fibrosis: Correlation of Biochemical, Physiological, and Histological Changes. Toxicology and Applied Pharmacology. 1981; 60:360–7. [PubMed: 6169174]
40. Holgate ST. Epithelium dysfunction in asthma. J Allergy Clin Immunol. 2007; 120:1233–1244. [PubMed: 18073119]
41. Holgate ST. The Airway Epithelium is Central to the Pathogenesis of Asthma. Allergology International. 2008; 57:1–10. [PubMed: 18209502]

42. Leino MS, Loxham M, Blume C, Swindle EJ, et al. Barrier Disrupting Effects of Alternaria Alternata Extract on Bronchial Epithelium from Asthmatic Donors. PLoS ONE. 2013; 8(8):e71278 (1–9). [PubMed: 24009658]
43. Zeki AA, Thai P, Kenyon NJ, Wu R. Differential effects of simvastatin on IL-13-induced cytokine gene expression in primary mouse tracheal epithelial cells. Respiratory Research. 2012; 13(1):38–46. [PubMed: 22583375]
44. Dunn SE, Youssef S, Goldstein MJ, Prod'homme T, Weber MS, Zamvil SS, Steinman L. Isoprenoids determine Th1/Th2 fate in pathogenic T cells, providing a mechanism of modulation of autoimmunity by atorvastatin. J Exp Med. 2006; 203(2):401–412. [PubMed: 16476765]
45. Chung KF. Targeting the interleukin pathway in the treatment of asthma. The Lancet. 2015; 386(9998):1086–1096.
46. Munitz A, Brandt EB, Mingler M, Finkelman FD, Rothenberg ME. Distinct roles for IL-13 and IL-4 via IL-13 receptor alpha1 and the type II IL-4 receptor in asthma pathogenesis. Proceedings of the National Academy of Sciences. 2008; 105(20):7240–7245.
47. Hebenstreit D, Wirnsberger G, Horejs-Hoeck J, Duschl A. Signaling mechanisms, interaction partners, and target genes of STAT6. Cytokine & Growth Factor Reviews. 2006; 17(3):173–188. [PubMed: 16540365]
48. Peng Q, Matsuda T, Hirst SJ. Signaling pathways regulating interleukin-13-stimulated chemokine release from airway smooth muscle. American Journal of Respiratory and Critical Care Medicine. 2004; 169(5):596–603. [PubMed: 14670803]
49. Thai P, Chen Y, Dolganov G, Wu R. Differential regulation of MUC5AC/Muc5ac and hCLCA-1/mGob-5 expression in airway epithelium. American Journal of Respiratory Cell and Molecular Biology. 2005; 33(6):523–530. [PubMed: 16151054]
50. Li L, Xia Y, Nguyen A, et al. Effects of Th2 cytokines on chemokine expression in the lung: IL-13 potently induces eotaxin expression by airway epithelial cells. Journal of Immunology. 1999; 162(5):2477–2487.
51. Hirst SJ, Hallsworth MP, Peng Q, Lee TH. Selective Induction of Eotaxin Release by Interleukin-13 or Interleukin-4 in Human Airway Smooth Muscle Cells Is Synergistic with Interleukin-1beta and Is Mediated by the Interleukin-4 Receptor alpha-Chain. Am J Respir Crit Care Med. 2002; 165(8):1161–1171. [PubMed: 11956062]
52. Lilly CM, Nakamura H, Kesselman H, et al. Expression of eotaxin by human lung epithelial cells. Induction by cytokines and inhibition by glucocorticoids. Journal of Clinical Investigation. 1997; 99(7):1767–1773. [PubMed: 9120022]
53. Ravensberg AJ, Ricciardolo FL, van Schadewijk A, Rabe KF, Sterk PJ, Hiemstra PS, Mauad T. Eotaxin-2 and eotaxin-3 expression is associated with persistent eosinophilic bronchial inflammation in patients with asthma after allergen challenge. J Allergy Clin Immunol. 2005; 115:779–785. [PubMed: 15805998]
54. Komiya A, Nagase H, Yamada H, Sekiya T, Yamaguchi M, Sano Y, Hanai N, Furuya A, Ohta K, Matsushima K, Yoshie O, Yamamoto K, Hirai K. Concerted expression of eotaxin-1, eotaxin-2, and eotaxin-3 in human bronchial epithelial cells. Cellular Immunology. 2003; 225:91–100. [PubMed: 14698143]
55. Larose MC, Chakir J, Archambault AS, et al. Correlation between CCL26 production by human bronchial epithelial cells and airway eosinophils: Involvement in patients with severe eosinophilic asthma. Journal of Allergy and Clinical Immunology. 2015; 136(4):904–913. [PubMed: 25936567]
56. Woodruff PG, Boushey H, Dolganov GM, et al. Genome-wide profiling identifies epithelial cell genes associated with asthma and with treatment response to corticosteroids. Proceedings of the National Academy of Sciences. 2007; 104(40):15858–15863.
57. Woodruff PG, Modrek B, Choy DF, et al. T-helper type 2-driven inflammation defines major subphenotypes of asthma. American Journal of Respiratory and Critical Care Medicine. 2009; 180(5):388–395. [PubMed: 19483109]
58. Cazzola M, Calzetta L, Page CP, Rinaldi B, Capuano A, Matera MG. Protein prenylation contributes to the effects of LPS on EFS-induced responses in human isolated bronchi. American Journal of Respiratory Cell and Molecular Biology. 2011; 45(4):704–710. [PubMed: 21278325]

59. Fessler MB. Regulation of Adaptive Immunity in Health and Disease by Cholesterol Metabolism. Current Allergy and Asthma Reports. 2015; 15(8):48. [PubMed: 26149587]
60. Thurnher M, Gruenbacher G. T lymphocyte regulation by mevalonate metabolism. Science Signaling. 2015; 8(370):re4. [PubMed: 25829448]
61. Chiba Y, Sato SS, Misawa M. Lovastatin inhibits antigen-induced airway eosinophilia without affecting the production of inflammatory mediators in mice. Inflammation Research. 2009; 58(7): 363–369. [PubMed: 19418204]
62. Scheele JS, Marks RE, Boss GR. Signaling by small GTPases in the immune system. Immunol Rev. 2007; 218:92–101. [PubMed: 17624946]
63. Popoff MR, Geny B. Multifaceted role of Rho, Rac, Cdc42 and Ras in intercellular junctions, lessons from toxins. Biochimica et Biophysica Acta. 2009; 1788(4):797–812. [PubMed: 19366594]
64. Downward J. Targeting Ras Signaling Pathways in Cancer Therapy. Nature Reviews. 2003; 3:11–22.
65. Sasaki O, Imamura M, Yamazumi Y, et al. Alendronate attenuates eosinophilic airway inflammation associated with suppression of Th2 cytokines, Th17 cytokines, and eotaxin-2. Journal of Immunology. 2013; 191(6):2879–2889.
66. Das S, Schapira M, Tomic-Canic M, Goyanka R, Cardozo T, Samuels HH. Farnesyl pyrophosphate is a novel transcriptional activator for a subset of nuclear hormone receptors. Molecular Endocrinology. 2007; 21(11):2672–2686. [PubMed: 17666588]
67. Maltese WA, Soule G, Gunning W, Calomeni E, Alexander B. Mutant Rab24 GTPase is targeted to nuclear inclusions. BMC Cell Biology. 2002; 3(1):25. [PubMed: 12323076]
68. Stenmark H. Rab GTPases as coordinators of vesicle traffic. Nat Rev Mol Cell Biol. 2009; 10(8): 513–525. [PubMed: 19603039]
69. Bhuin T, Kumar J. Rab proteins: The key regulators of intracellular vesicle transport. Experimental cell research. 2014; 328:1–19. [PubMed: 25088255]
70. Hutagalung AH, Novick PJ. Role of Rab GTPases in Membrane Traffic and Cell Physiology. Physiol Rev. 2011; 91:119–149. [PubMed: 21248164]
71. Leung KF, Baron R, Seabra MC. Geranylgeranylation of Rab GTPases. Journal of Lipid Research. 2006; 47:467–475. [PubMed: 16401880]
72. Hakamada-taguchi R, Uehara Y, Kuribayashi K, et al. Inhibition of Hydroxymethylglutaryl-Coenzyme A Reductase Reduces Th1 Development and Promotes Th2 Development. Circulation. 2016; 93:948–956.
73. Waiczies S, Bendix I, Zipp F. Immunology Not GTP-Loading of Rho GTPases Determines T Cell Function. Science Signaling. 2008; 1(pt3):1–4.
74. Ghittoni R, Patrussi L, Pirozzi K, Pellegrini M, Lazzerini PE, Capecchi PL, Pasini FL, Baldari CT. Simvastatin inhibits T-cell activation by selectively impairing the function of Ras superfamily GTPases. FASEB J. 2005; 19(6):605–607. [PubMed: 15677697]
75. Imamura M, Okunishi K, Ohtsu H, Nakagome K, Harada H, Tanaka R, Yamamoto K, Dohi M. Pravastatin attenuates allergic airway inflammation by suppressing antigen sensitization, interleukin 17 production and antigen presentation in the lung. Thorax. 2009; 64:44–49. [PubMed: 18835962]
76. Xue X, Lai KA, Huang J, Gu Y, Karlsson L, Fourie A. Anti-Inflammatory Activity in Vitro and in Vivo of the Protein Farnesyltransferase Inhibitor Tipifarnib. Journal of Pharmacology and Experimental Therapeutics. 2006; 317(1):53–60. [PubMed: 16352705]
77. Albeck JG, Mills GB, Brugge JS. Frequency-Modulated Pulses of ERK Activity Transmit Quantitative Proliferation Signals. Molecular Cell. 2013; 49(2):249–261. [PubMed: 23219535]
78. Agudo-Ibáñez L, Herrero A, Barbacid M, Crespo P. H-Ras distribution and signaling in plasma membrane microdomains are regulated by acylation and deacylation events. Molecular and Cellular Biology. 2015; 35(11):1898–1914. [PubMed: 25776558]
79. Papke, B., Schmick, M., Vartak, N., Bastiaens, PIH. Ras Superfamily Small G Proteins: Biology and Mechanisms I. 2014. Chapter 8: The Spatial Organization of Ras Signaling; p. 173-188.
80. Bunda S, Heir P, Srikumar T, et al. Src promotes GTPase activity of Ras via tyrosine 32 phosphorylation. Proceedings of the National Academy of Sciences. 2014; 111(36):E3785–E3794.

81. Charron G, Li MMH, MacDonald MR, Hang HC. Prenylome profiling reveals S-farnesylation is crucial for membrane targeting and antiviral activity of ZAP long-isoform. Proceedings of the National Academy of Sciences. 2013; 110(27):11085–11090.
82. Vukelic S, Stojadinovic O, Pastar I, et al. Farnesyl pyrophosphate inhibits epithelialization and wound healing through the glucocorticoid receptor. The Journal of Biological Chemistry. 2010; 285(3):1980–1988. [PubMed: 19903814]
83. Lerner EC, Qian Y, Blaskovich MA, et al. Ras CAAX Peptidomimetic FTI-277 Selectively Blocks Oncogenic Ras Signaling by Inducing Cytoplasmic Accumulation of Inactive Ras-Raf Complexes. Journal of Biological Chemistry. 1995; 270(45):26802–26806. [PubMed: 7592920]
84. Lerner EC, Zhang T, Knowles DB, Qian Y, Hamilton AD. Inhibition of the prenylation of K-Ras, but not H- or N-Ras, is highly resistant to CAAX peptidomimetics and requires both a farnesyltransferase and a geranylgeranyltransferase I inhibitor in human tumor cell lines. Oncogene. 1997; 15:1283–1288. [PubMed: 9315095]
85. Pelaia G, Gallelli L, Renda T, et al. Effects of statins and farnesyl transferase inhibitors on ERK phosphorylation , apoptosis and cell viability in non-small lung cancer cells. Cell Proliferation. 2012; 45:557–565. [PubMed: 23045963]
86. Sebti SM, Hamilton AD. Farnesyltransferase and geranylgeranyltransferase I inhibitors and cancer therapy: Lessons from mechanism and bench-to-bedside translational studies. Oncogene. 2000; 19:6584–6593. [PubMed: 11426643]
87. Cox AD, Der CJ. Farnesyltransferase inhibitors: promises and realities. Current Opinion in Pharmacology. 2002; 2:388–393. [PubMed: 12127871]
88. Lobell RB, Omer CA, Abrams MT, et al. Evaluation of Farnesyl: Protein Transferase and Geranylgeranyl:Protein Transferase Inhibitor Combinations in Preclinical Models. Cancer Res. 2001; 61:8758–8768. [PubMed: 11751396]
89. Lee KH, Koh M, Moon A. Farnesyl transferase inhibitor FTI-277 inhibits breast cell invasion and migration by blocking H-Ras activation. Oncology Letters. 2016; 12(3):2222–2226. [PubMed: 27602167]
90. Bates ME, Sedgwick JB, Zhu Y, et al. Human Airway Eosinophils Respond to Chemoattractants with Greater Eosinophil-Derived Neurotoxin Release, Adherence to Fibronectin, and Activation of the Ras–ERK Pathway When Compared with Blood Eosinophils. Journal of Immunology. 2010; 184:7125–7133.
91. Whyte DB, Kirschmeier P, Hockenberry TN, et al. K- and N-Ras Are Geranylgeranylated in Cells Treated with Farnesyl Protein Transferase Inhibitors. The Journal of Biological Chemistry. 1997; 272(22):14459–14464. [PubMed: 9162087]
92. Basso AD, Kirschmeier P, Bishop WR. Farnesyl transferase inhibitors. Journal of Lipid Research. 2006; 47:15–31. [PubMed: 16278491]
93. Omerovic J, Prior IA. Compartmentalized signalling: Ras proteins and signalling nanoclusters. FEBS Journal. 2009; 276:1817–1825. [PubMed: 19243428]
94. Aicart-Ramos C, Valero RA, Rodriguez-Crespo I. Protein palmitoylation and subcellular trafficking. Biochimica et Biophysica Acta - Biomembranes. 2011; 1808(12):2981–2994.
95. Koarai A, Yanagisawa S, Sugiura H, et al. 25-Hydroxycholesterol enhances cytokine release and Toll-like receptor 3 response in airway epithelial cells. Respiratory Research. 2012; 13:63. [PubMed: 22849850]
96. Rezen T, Rozman D, Pascussi JM, Monostory K. Interplay between cholesterol and drug metabolism. Biochimica et Biophysica Acta - Proteins and Proteomics. 2011; 1814(1):146–160.
97. Zhuravliova E, Barbakadze T, Narmania N, Ramsden J, Mikeladze D. Inhibition of nitric oxide synthase and farnesyltransferase change the activities of several transcription factors. Journal of Molecular Neuroscience. 2007; 31(3):281–287. [PubMed: 17726232]
98. Roberts PJ, Mitin N, Keller PJ, et al. Rho family GTPase modification and dependence on CAAX motif-signaled posttranslational modification. Journal of Biological Chemistry. 2008; 283(37): 25150–25163. [PubMed: 18614539]
99. Wang XH, Wang Y, Diao F, Lu J. RhoB is involved in lipopolysaccharide-induced inflammation in mouse in vivo and in vitro. Journal of Physiology and Biochemistry. 2013; 69(2):189–197. [PubMed: 22869204]

100. Luis-Ravelo D, Anton I, Zandueta C, et al. RHOB influences lung adenocarcinoma metastasis and resistance in a host-sensitive manner. Molecular Oncology. 2014; 8(2):196–206. [PubMed: 24321314]

101. Wojciak-Stothard B, Zhao L, Oliver E, et al. Role of RhoB in the regulation of pulmonary endothelial and smooth muscle cell responses to hypoxia. Circulation Research. 2012; 110(11): 1423–1434. [PubMed: 22539766]

102. Li J, Herold MJ, Kimmel B, et al. Reduced expression of the mevalonate pathway enzyme farnesyl pyrophosphate synthase unveils recognition of tumor cells by Vgamma9Vdelta2 T cells. Journal of Immunology. 2009; 182(12):8118–8124.

103. Spencer CT, Abate G, Blazevic A, Hoft DF. Only a Subset of Phosphoantigen-Responsive delta9-gamma2 T Cells Mediate Protective Tuberculosis Immunity. The Journal of Immunology. 2016; 181(7):4471–4484.

104. Dieli F, Fadda R, Caccamo N. Butyrophilin 3A1 presents phosphoantigens to human γδ T cells: the fourth model of antigen presentation in the immune system. Cellular & Molecular Immunology. 2014; 11(2):123–125. [PubMed: 24270471]

105. Champagne E. Gamma-Delta T cell receptor ligands and modes of antigen recognition. Archivum Immunologiae et Therapiae Experimentalis. 2011; 59(2):117–137. [PubMed: 21298486]

106. Kabelitz D, Dechanet-Merville J. Editorial: “Recent advances in gamma/delta T cell biology: new ligands, new functions, and new translational perspectives”. Frontiers in Immunology. 2015; 6:371(4–9). [PubMed: 26257738]

107. De Libero G. Sentinel function of broadly reactive human gamma delta T cells. Immunology Today. 1997; 18(1):22–26. [PubMed: 9018970]

108. Karunakaran MM, Herrmann T. The V9V2 T cell antigen receptor and butyrophilin-3 A1: Models of interaction, the possibility of co-evolution, and the case of dendritic epidermal T cells. Frontiers in Immunology. 2014; 5:1–13. [PubMed: 24474949]

109. Rhodes DA, Chen H-C, Price AJ, et al. Activation of Human γδ T Cells by Cytosolic Interactions of BTN3A1 with Soluble Phosphoantigens and the Cytoskeletal Adaptor Periplakin. Journal of Immunology. 2015; 194(5):2390–2398.

110. De Libero G, Lau SY, Mori L. Phosphoantigen presentation to TCR gamma-delta cells, a conundrum getting less gray zones. Frontiers in Immunology. 2015; 5:679 (1–10). [PubMed: 25642230]

111. Ullah MA, Revez JA, Loh Z, et al. Allergen-induced IL-6 trans-signaling activates γδ T cells to promote type 2 and type 17 airway inflammation. Journal of Allergy and Clinical Immunology. 2015; 136(4):1065–1073. [PubMed: 25930193]

112. Morita CT, Lee HK, Wang H, Li H, Mariuzza RA, Tanaka Y. Structural features of nonpeptide prenyl pyrophosphates that determine their antigenicity for human gamma delta T cells. Journal of Immunology. 2001; 167(1):36–41.

113. Zeki AA, Bratt JM, Chang KY, et al. Intratracheal instillation of pravastatin for the treatment of murine allergic asthma: a lung-targeted approach to deliver statins. Physiological Reports. 2015; 3(5):e12352–e12352. [PubMed: 25969462]

114. Xu L, Dong X, Shen L, et al. Simvastatin delivery via inhalation attenuates airway inflammation in a murine model of asthma. International Immunopharmacology. 2012; 12(4):556–564. [PubMed: 22326624]

115. Tulbah AS, Ong HX, Colombo P, Young PM, Traini D. Novel Simvastatin Inhalation Formulation and Characterisation. AAPS PharmSciTech. 2014; 15(4):956–962. [PubMed: 24806822]

116. Tulbah AS, Ong HX, Morgan L, Colombo P, Young PM, Traini D. Dry powder formulation of simvastatin. Expert Opin Drug Deliv. 2015; 12(6):857–868. [PubMed: 25244365]

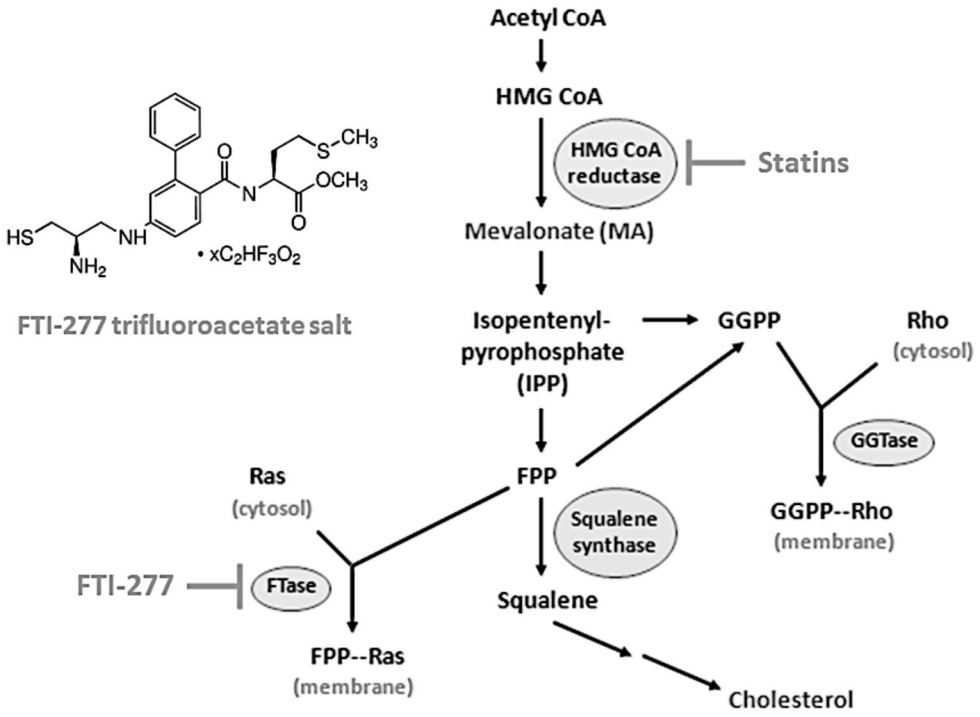

Figure 1. The mevalonate (MA) pathway

Previous work has established that inhibition of HMGCR with a statin drug significantly reduces eosinophilic airway inflammation and AHR in experimental allergic asthma. To further elucidate the role of the FTase arm of the MA pathway in mediating type 2/Th2 inflammation, we utilized FTI-277 to inhibit FTase enzyme activity. GGTase and squalene synthase are the alternate arms of the MA pathway but were not assessed in this study. The chemical structure of the FTase inhibitor FTI-277 (a Ras CaaX motif peptidomimetic) is shown in the inset.

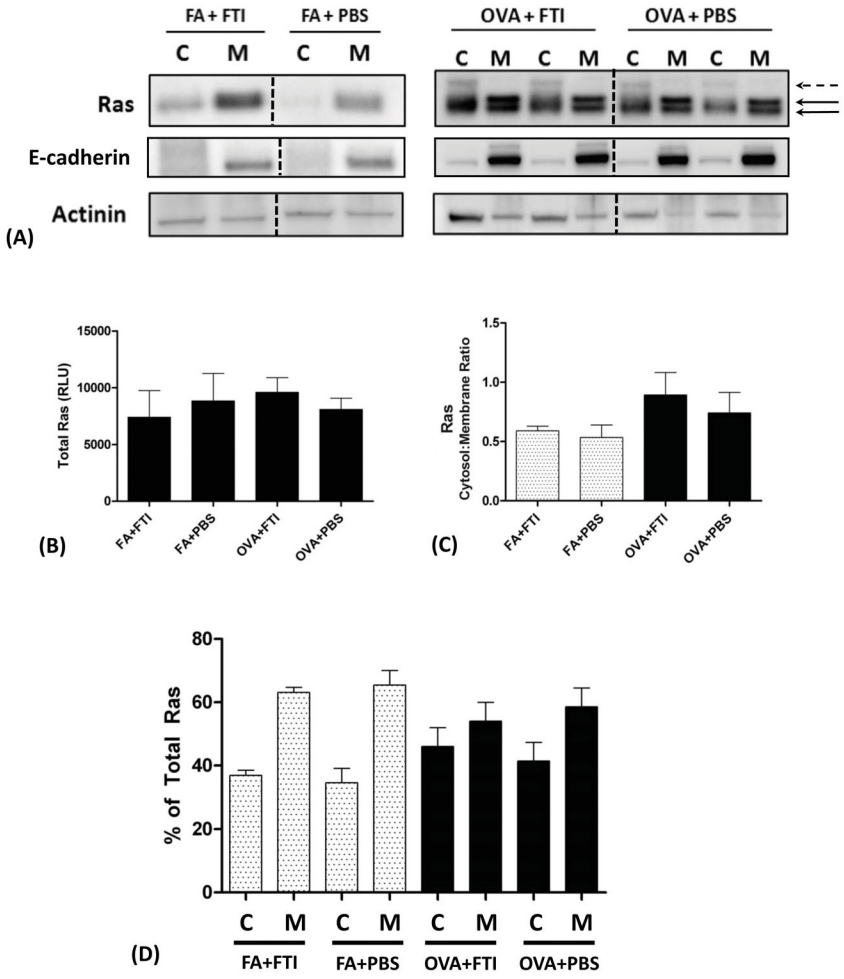

Figure 2. Subcellular Localization of Ras in Air- and Allergen-Exposed Mice and the Effects of FTI-277 Treatment on Ras Subcellular Translocation

BALB/c mice were sensitized to ovalbumin (OVA) and then challenged with 1% OVA aerosol or filtered air six times over a 2-week period. Mice were injected daily with FTI-277 (20 mg/kg/day, i.p.) before each OVA aerosol exposure. Whole lung homogenates were processed into cytosolic [C] and membrane [M] subcellular fractions, and Ras protein expression in these fractions was assessed by Western blot. Ras semi-quantitative values were normalized using E-cadherin and actinin for membrane and cytosolic fractions, respectively.

(A) In mice exposed to FA, Ras resides predominantly in the [M] fraction. With OVA exposure, Ras becomes nearly evenly distributed between the [C] and [M] fractions. These data indicated that under basal non-inflamed conditions, Ras is farnesylated and membrane-bound. All [C] bands represent unfarnesylated Ras including the faint band above the lowest one (dashed black arrow), and the [M] bands represent farnesylated membrane-anchored Ras (solid black arrows).

The dashed black vertical lines represent the space where images of bands were joined from a single blot to show the representative bands shown here. All relevant bands (and blots),

including the representative bands above, were used to generate and analyze the data shown in panels B–D.

(B) Total Ras protein expression did not differ with FTI-277 treatment for both the FA and OVA groups (p=NS by 1-way ANOVA).

(C) Plotted as cytosol-to-membrane ratio, treatment with FTI-277 did not affect Ras translocation in both FA and OVA groups (p=NS by 1-way ANOVA).

(D) Plotted as % of total Ras, treatment with FTI-277 showed no statistically significant changes in [C]- or [M]-associated Ras in both FA and OVA groups (p=NS by 1-way ANOVA). Similarly, there were no significant changes in [C] or [M] subcellular fractions in PBS controls for both FA and OVA groups (p=NS by 1-way ANOVA).

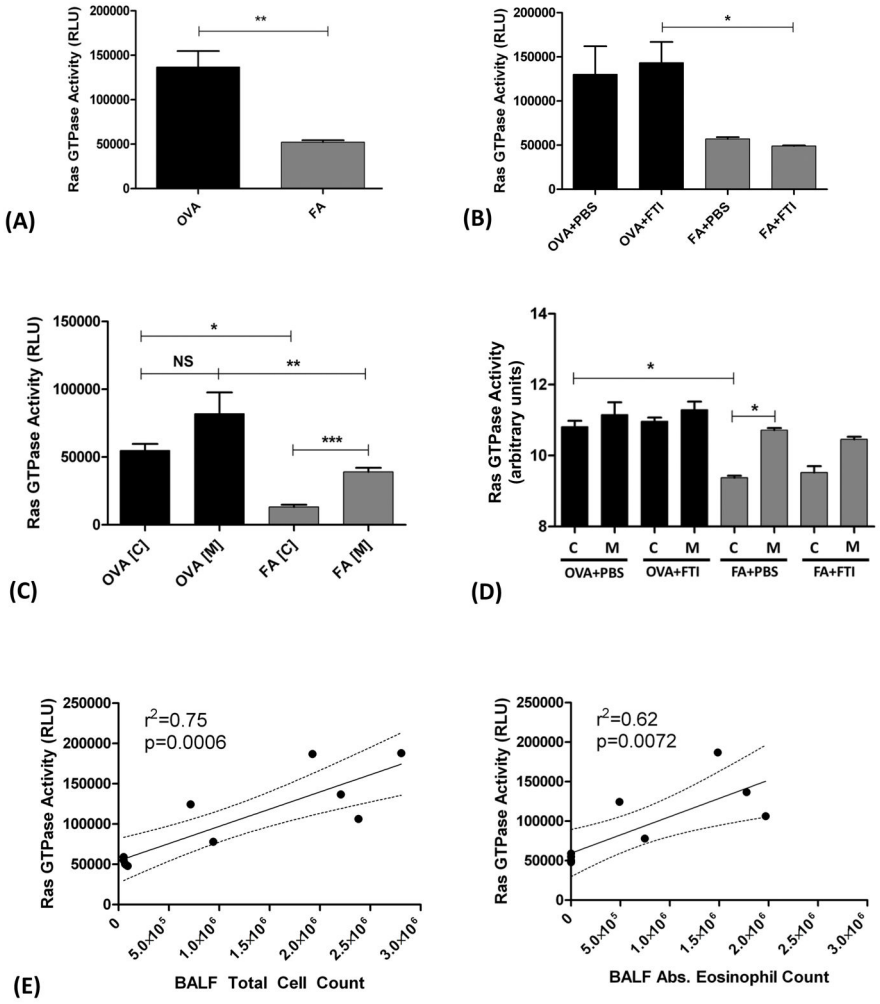

Figure 3. Effect of FTI-277 Treatment on Ras GTPase Activity in Mouse Lung

BALB/c mice were sensitized to ovalbumin (OVA) and then challenged with 1% OVA aerosol or filtered air six times over a 2-week period. Mice were injected daily with FTI-277 (20 mg/kg/day, i.p.) before each OVA aerosol exposure. Ras GTPase activity was measured in whole lung homogenates, and in cytosolic [C] and membrane [M] subcellular fractions. Ras GTPase enzymatic activity was measured by ELISA.

(A) In unfractionated whole lung homogenate tissue, OVA-exposed mice have 2.61-fold greater total Ras GTPase activity compared to FA controls (**p=0.0022 by *t test*).

(B) FTI-277 treatment had no effect on Ras GTPase activity in either FA or OVA-exposed mice (p=NS by 1-way ANOVA). The OVA groups have greater Ras activity than the FA control groups (2.28-fold difference in OVA+PBS vs. FA+PBS, p=NS; and 2.92-fold difference in OVA+FTI vs. FA+FTI *p<0.05 by 1-way ANOVA).

(C) Comparing groups by subcellular fraction, Ras GTPase activity is higher in the cell [M] fractions as compared to [C] fractions for both the OVA and FA groups (OVA[C] vs. OVA[M], p=NS; FA[C] vs. FA[M], ***p<0.001, by 1-way ANOVA). In both the [C] and [M] fractions comparing OVA vs. FA, Ras GTPase activity was significantly greater in the

OVA groups (OVA[C] vs. FA[C], *p<0.05; OVA[M] vs. FA[M], **p<0.01 by 1-way ANOVA).

(D) In OVA-exposed mice, treatment with FTI-277 did not affect Ras enzyme activity in the membrane [M] or cytosolic [C] fractions for both groups (OVA+PBS [C] vs. [M] and OVA +FTI [C] vs. [M], p=NS for all comparisons by 1-way ANOVA). Ras GTPase activity in the [C] fraction of the OVA+PBS group was significantly higher than the FA+PBS control (OVA +PBS [C] vs. FA+PBS [C], *p<0.01 by 1-way ANOVA). The [M] fraction had a significantly greater Ras GTPase activity as compared to the [C] fraction in the FA+PBS group (FA+PBS [C] vs. FA+PBS [M], *p<0.05 by 1-way ANOVA), but this effect was only a trend in the FTI-277-treated FA mice (FA+FTI [C] vs. FA+FTI [M], p=NS by 1-way ANOVA). *Note: Ras GTPase activity units were natural log transformed prior to analysis. The graph shows transformed data and therefore displays arbitrary units.*

(E) Ras GTPase activity demonstrated a positive linear correlation with BALF total inflammatory cell count (r^2=0.75, p=0.0006, confidence interval (CI) 0.0239 to 0.0615) and with BALF absolute (abs.) eosinophil count (r^2=0.62, p=0.0072, CI 0.0165 to 0.076). *Note: Total Ras activity of combined membrane (M) and cytosol (C) fractions are plotted.*

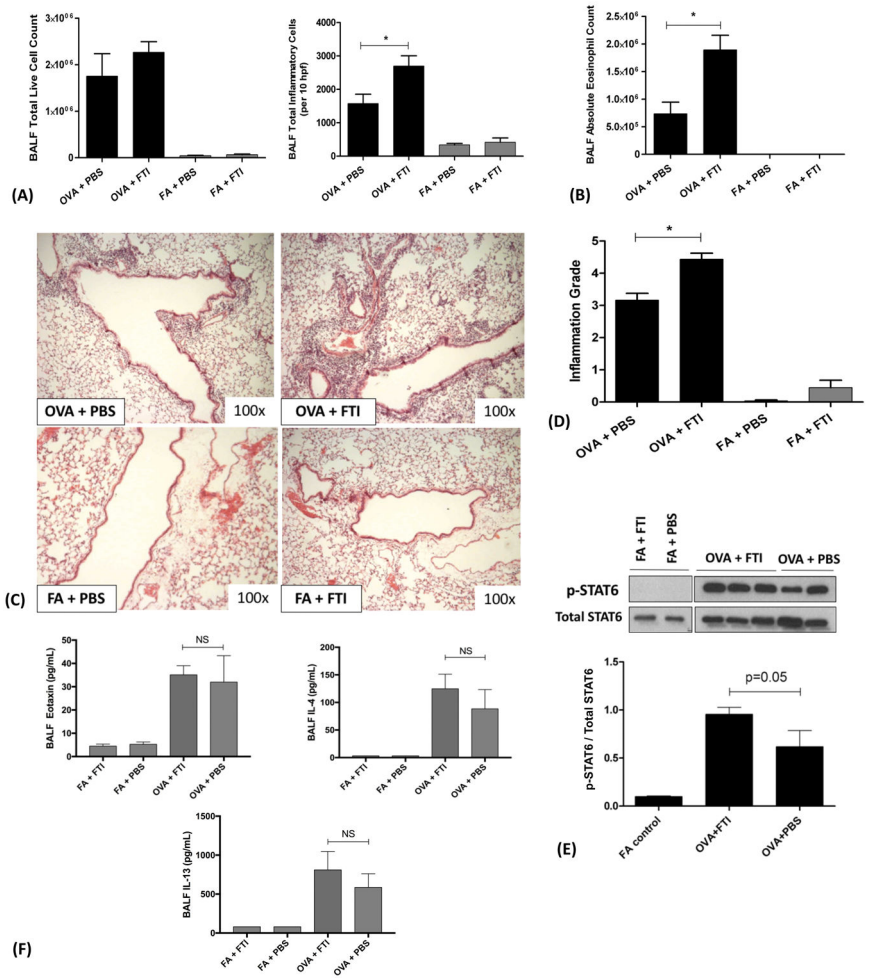

Figure 4. FTase Inhibition with FTI-277 Exacerbates Allergic Airway Inflammation in a IL4/IL13/STAT6/eotaxin-Independent Manner

BALB/c mice were sensitized to ovalbumin (OVA) and then challenged with 1% OVA aerosol or filtered air six times over a 2-week period. Mice were injected daily with FTI-277 (20 mg/kg/day, i.p.) before each OVA aerosol exposure. To assess for inflammation and drug effect, we quantified total and differential inflammatory cell counts and chemokines/cytokines in BALF, assessed histopathology and Inflammation Grade by H&E staining, and measured total- and phosphorylated STAT6 in whole lung homogenate by Western blot.

(A) In OVA-exposed mice, treatment with FTI-277 did not significantly increase BALF total live cell count (p=NS by 1-way ANOVA). However, measured as BALF total inflammatory cells/per 10 hpf, FTI-277 treatment of OVA-exposed mice increased inflammatory cell influx by 1.72-fold with (*p<0.05, by 1-way ANOVA). Treatment with FTI-277 had no detectible pro-inflammatory effects in any of the FA control groups.

(B) Treatment with FTI-277 increased BALF absolute eosinophil count by 2.58-fold, (OVA +PBS vs. OVA+FTI, *p<0.01 by 1-way ANOVA).

(C) H&E stained lung sections indicate that treatment with FTI-277 augmented peribronchial and perivascular inflammation in the OVA-exposed mice.

(D) Semi-quantification of the H&E sections corresponded to a 1.40-fold increase in the Inflammation Grade (*p<0.001, by 1-way ANOVA). There were no statistically significant effects of FTI-277 on Inflammation Grade in the FA-exposed control groups.
(E) In OVA-exposed mice, there was a significant increase in STAT6 phosphorylation as compared to FA controls. Treatment with FTI-277 further increased OVA-induced STAT6 phosphorylation by 1.55-fold, but this was not statistically significant (OVA+PBS vs. OVA +FTI, p=0.05, by 1-way ANOVA).
(F) Cytokines IL4 and IL13 induce phosphorylation of the transcription factor STAT6 which then activates the transcription of eotaxin. To assess this, we measured peptide levels of secreted IL4, IL13, and eotaxin in BALF. There were no statistically significant differences in BALF eotaxin levels (p=NS, by 1-way ANOVA) with FTI-277 treatment in either FA or OVA groups. The cytokine IL-4 was significantly induced in BALF upon OVA exposure (OVA+FTI vs. FA+FTI, p=0.0371 by 1-way ANOVA), however, there were no statistically significant differences in BALF IL-4 levels with FTI-277 treatment in either FA or OVA groups (p=NS, by 1-way ANOVA). There were no statistically significant differences in BALF IL-13 levels with FTI-277 treatment in either FA or OVA groups (p=NS, by 1-way ANOVA).

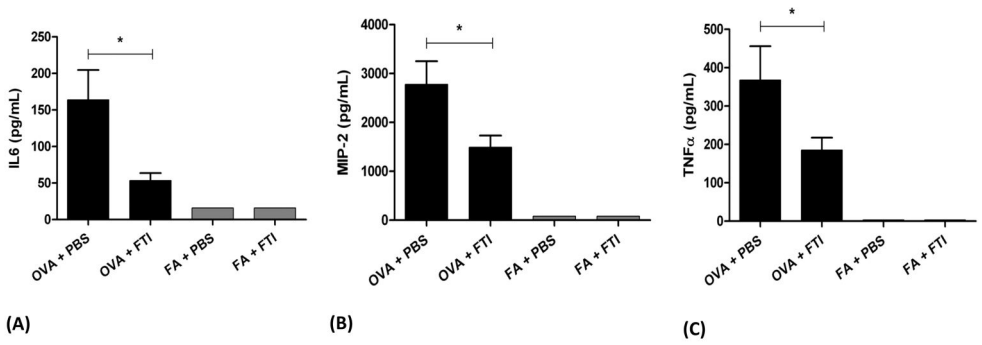

Figure 5. Effect of FTI-277 on Select BALF Cytokine Levels

BALB/c mice were sensitized to ovalbumin (OVA) and then challenged with 1% OVA aerosol or filtered air six times over a 2-week period. Mice were injected daily with FTI-277 (20 mg/kg/day, i.p.) before each OVA aerosol exposure. BALF supernatant was collected for multiplex analysis for select cytokines and chemokines. Treatment with FTI-277 reduced cytokine levels of IL-6, MIP-2, and TNFα (see the **Results** section for the rest of the cytokine/chemokine measures, which did not reach significance).

In the OVA group, treatment with FTI-277 reduced cytokine concentrations in BALF by the following amounts: **(A)** IL6 by 67.4% (*p=0.0258), **(B)** MIP-2 by 46.3% (*p=0.0356), and **(C)** TNFα by 49.6% (*p=0.05), all analyzed by 1-way ANOVA. There were no significant changes in the FA control groups.

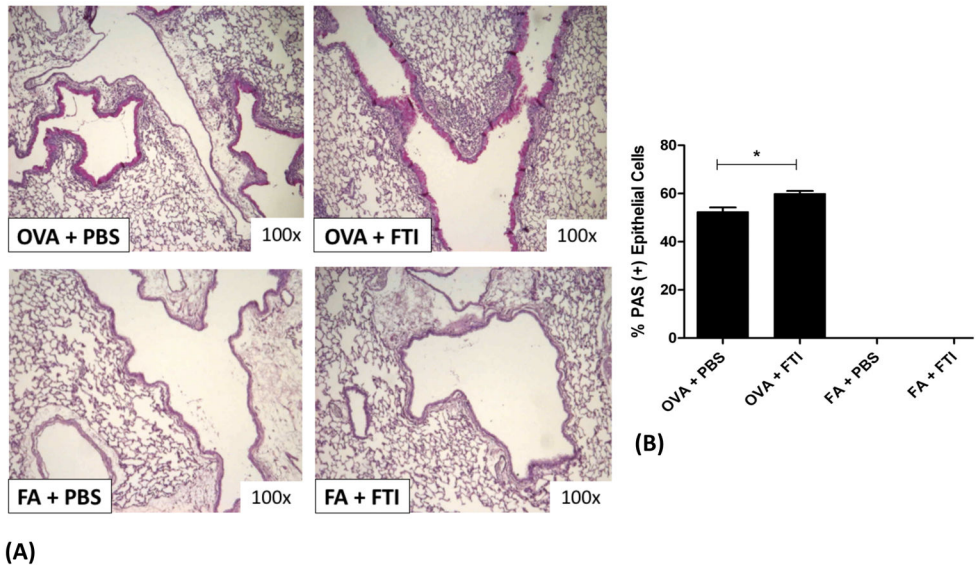

Figure 6. FTase Inhibition with FTI-277 Increases Airway Goblet Cell Hyperplasia

BALB/c mice were sensitized to ovalbumin (OVA) and then challenged with 1% OVA aerosol or filtered air six times over a 2-week period. Mice were injected daily with FTI-277 (20 mg/kg/day, i.p.) before each OVA aerosol exposure. PAS staining of lung sections was used to assess the degree of goblet cell metaplasia/hyperplasia as a measure of airway epithelial remodeling and mucus production.

(A) PAS staining of lung sections showed that treatment with FTI-277 further increases OVA-induced goblet cell metaplasia/hyperplasia in the airway epithelium.

(B) The proportion of %PAS positive airway epithelial cells increased by 1.14-fold (*p=0.025 by *t test*) with FTI-277 treatment as compared to OVA+PBS controls. There were virtually no goblet cells present in the conducting airways of mice exposed to FA in both the PBS and FTI-277-treated groups.

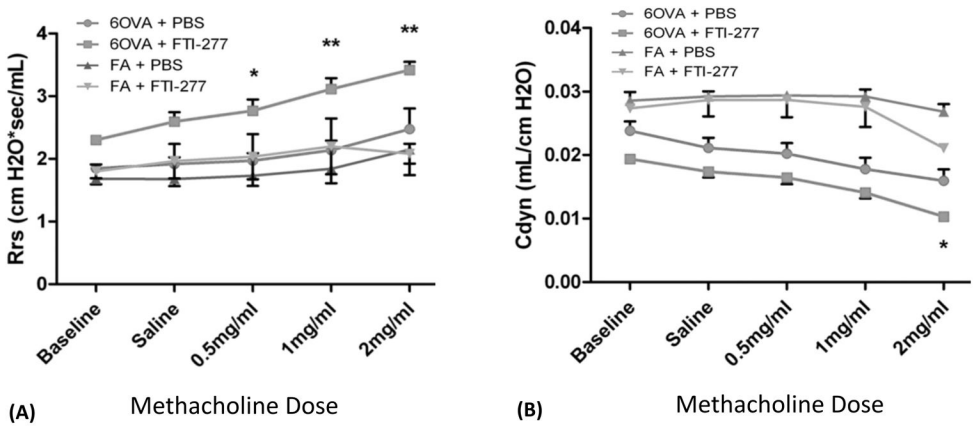

Figure 7. FTase Inhibition with FTI-277 Exacerbates Airway Hyperreactivity (AHR) and Decreases Lung Compliance

BALB/c mice were sensitized to ovalbumin (OVA) and then challenged with 1% OVA aerosol or filtered air six times over a 2-week period. Mice were injected daily with FTI-277 (20 mg/kg/day, i.p.) before each OVA aerosol exposure. Before and after increasing doses of methacholine (MCh), lung physiology was measured in all treatment groups to assess the effects of FTI-277 treatment on respiratory function.

(A) There were no significant baseline differences in Rrs between OVA+PBS vs. OVA+FTI (p=NS by 2-way ANOVA). Treatment with FTI-277 increased respiratory system resistance (Rrs) and AHR at all three doses of MCh (*p<0.05 for OVA+PBS vs. OVA+FTI; **p<0.01 for OVA+PBS vs. OVA+FTI). The greatest difference in Rrs was seen between OVA+PBS vs. OVA+FTI at the highest dose of MCh (2 mg/mL). There were no statistically significant differences in Rrs in FA controls ± FTI-277 treatment (FA + PBS vs. FA + FTI, p=NS).

(B) There were no baseline differences in Cdyn between OVA+PBS vs. OVA+FTI (p=NS by 2-way ANOVA). Treatment with FTI-277 decreases dynamic lung compliance (Cdyn) (*p<0.05 for OVA+PBS vs. OVA+FTI) at the highest dose of MCh (2 mg/mL). There were no statistically significant differences in Cdyn in FA controls ± FTI treatment (FA + PBS vs. FA + FTI, p=NS).

NOTE: All analyses were done by 2-way ANOVA with post-test corrections.

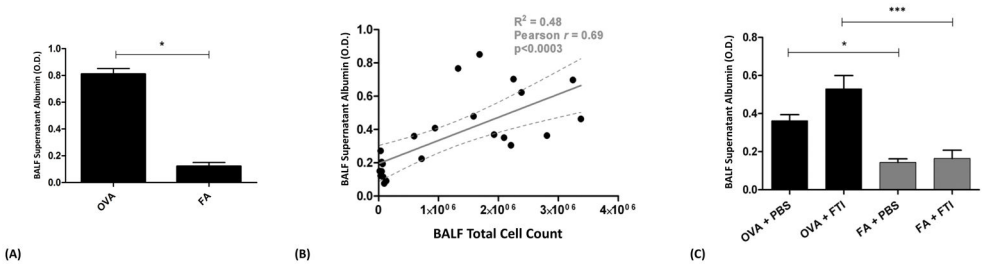

Figure 8. The Effects of FTI-277 Treatment on Alveolar-Capillary Membrane (ACM) Barrier Integrity

BALB/c mice were sensitized to ovalbumin (OVA) and then challenged with 1% OVA aerosol or filtered air six times over a 2-week period. Mice were injected daily with FTI-277 (20 mg/kg/day, i.p.) before each OVA aerosol exposure. We measured BALF albumin concentration as an indicator of ACM barrier health in our model, and to assess for endothelial or epithelial toxicity due to FTI-277. Data are represented as optical density (O.D.) at a wavelength of 450 nm.

(A) Sensitization followed by exposure to nebulized OVA alone induces vascular leak of albumin into the alveolar compartment indicating relative ACM barrier injury. OVA-exposed mice had a 6.7-fold increase of albumin in OVA- compared to FA-exposed mice (*p=0.0055 by *t test*).

(B) BALF supernatant albumin levels positively correlate with BALF total cell count ($p<0.0003$, $r^2=0.48$, Pearson $r=0.69$, 95% Confidence Interval of 7.3×10^{-8} to 2.04×10^{-7}).

(C) Treatment with FTI-277 does not result in a statistically significant change in BALF albumin levels in both the OVA and FA groups (OVA+PBS vs. OVA+FTI, and FA+PBS vs. FA+FTI, p=NS by 1-way ANOVA for both comparisons). Similar to panel (A), the OVA groups had significantly higher levels of BALF albumin independent of FTI treatment (OVA +PBS vs. FA+PBS, *p<0.05 by 1-way ANOVA; OVA+FTI vs. FA+FTI, ***p<0.001 by 1-way ANOVA). These data indicate that FTI-277 treatment alone did not independently compromise ACM barrier integrity.

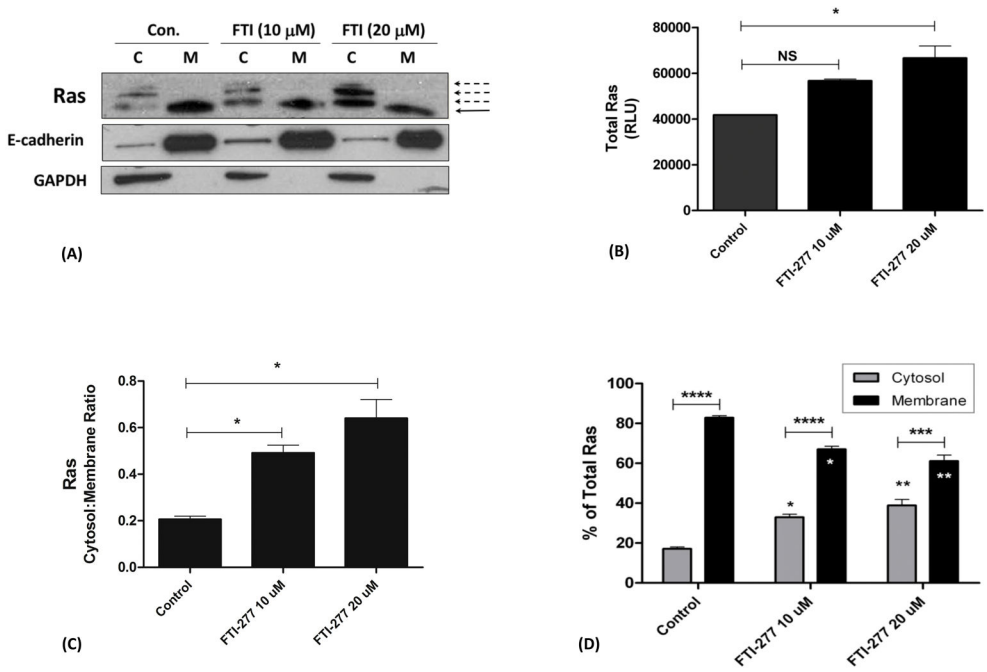

Figure 9. Subcellular Localization of Ras in HBE1 Cells and the Effects of FTI-277 Treatment

HBE1 human bronchial epithelial cells were treated with FTI-277 (10 and 20 μM) or control drug vehicle for 30 minutes. Cell homogenates underwent high speed ultra-centrifugation to separate them into cytosolic [C] and membrane [M] subcellular fractions. Ras protein for each treatment group was assessed by Western blot. Ras semi-quantitative values were normalized using E-cadherin and GAPDH for membrane and cytosolic fractions, respectively. A total of n=3 independent experiments were conducted of which a representative gel is shown. *Abbreviations: C=cytosol, M=membrane, FTI=FTI-277.*

(A) In the untreated control, Ras protein is highly expressed and is localized predominantly in the cell membrane fraction (solid black arrow). Treatment with FTI-277 increases Ras protein in the [C] fraction while decreasing Ras in the [M] fraction in a dose-dependent manner. The additional bands seen in the [C] fractions represent increasing proportions of unfarnesylated Ras protein with increasing FTI-277 dose (dashed black arrows).

(B) Treatment with FTI-277 caused a dose-dependent increase in total Ras protein expression (Control vs. FTI 10 μM (p=NS); Control vs. FTI 20 μM (*p<0.05 by 1-way ANOVA)).

(C) Plotted as cytosol-to-membrane ratio, the [C] fraction of Ras increased relative to the [M] fraction with increasing doses of FTI-277 (Control vs. FTI 10 μM, *p=0.02; Control vs. FTI 20 μM, *p=0.02, by 1-way ANOVA).

(D) Plotted as % of total Ras, treatment with FTI-277 resulted in a statistically significant increase in cytosolic Ras corresponding with a decrease in membrane-associated Ras. Cytosol vs. Membrane comparisons for each treatment group showed the following: Control (****p<0.0001 by 2-way ANOVA), FTI 10 μM (****p<0.0001), and FTI 20 μM (***p<0.001). For [C] and [M] comparisons across each treatment group, respectively: Control vs. FTI 10 μM (*p<0.05 by 1-way ANOVA), Control vs. FTI 20 μM (**p=0.0098), and FTI 10 μM vs. FTI 20 μM (p=NS)).

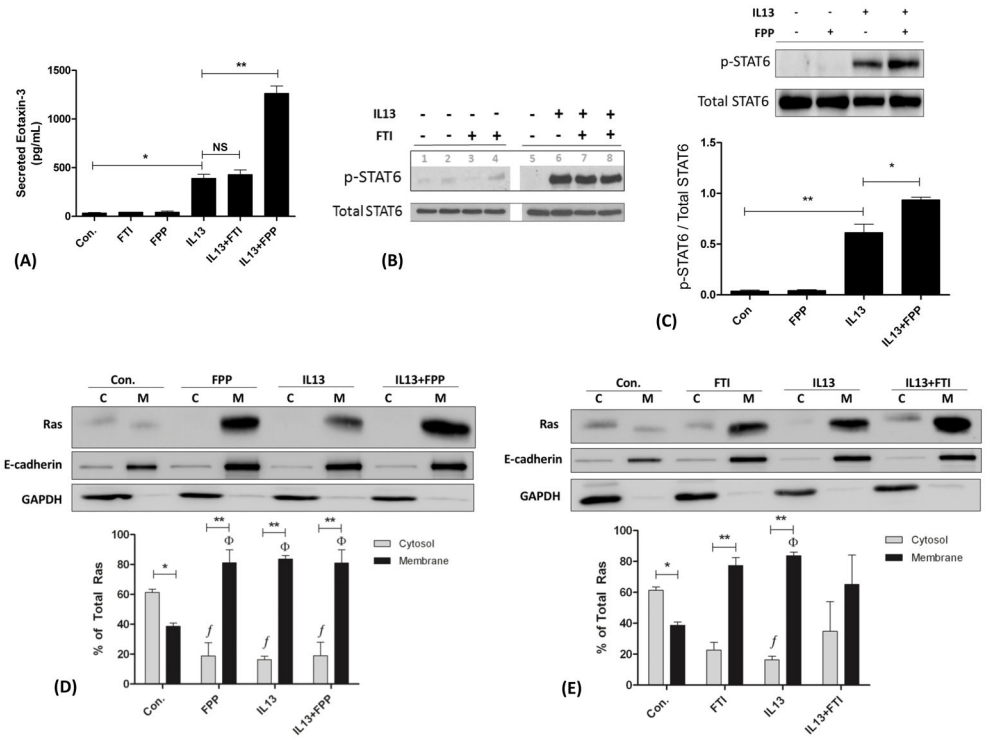

Figure 10. Effects of FTI-277 and FPP on IL13-Induced Eotaxin-3 Secretion and STAT6 Phosphorylation in HBE1 Cells

HBE1 human bronchial epithelial cells were pre-treated with FTI-277 (5, 10, or 20 μM) or FPP (10 μM) for 60 hours, then stimulated with IL13 for another 12 hours (72 hours total). Cell-free media were then collected to measure secreted eotaxin-3 peptide by ELISA. Total cell homogenates were collected for total- and p-STAT6, and cell membrane [M] and cytosolic [C] subcellular fractions for Ras expression by Western blot. Ras semi-quantitative values were normalized using E-cadherin and GAPDH for membrane and cytosolic fractions, respectively. A total of n=3 independent experiments were conducted of which representative gels are shown. *Abbreviations: C=cytosol, M=membrane, FTI=FTI-277.*

(A) Stimulation of HBE1 cells with IL13 resulted in an 11.3-fold increase in eotaxin-3 secretion (Control vs. IL13, *p<0.001 by 1-way ANOVA). Pre-treatment of HBE1 cells with FTI-277 (20 μM) did not affect IL13-induced eotaxin-3 secretion (p=NS). While exposure to FPP (10 μM) by itself had no effect on basal eotaxin-3 production, FPP augmented IL13-induced eotaxin-3 secretion by 3.2-fold (IL13 vs. IL13+FPP, **p<0.001 by 1-way ANOVA).

(B) Stimulation of HBE1 cells with IL13 induced STAT6 phosphorylation (p-STAT6). Pre-treatment with FTI-277 (5 and 10 μM) did not affect STAT6 phosphorylation. Gel lanes 3 and 7 were treated with 5 μM of FTI-277. Gel lanes 4 and 8 were treated with 10 μM of FTI-277.

(C) Stimulation of HBE1 cells with IL13 caused a 16.3-fold increase in p-STAT6 relative to total STAT6 (**p<0.01 by 1-way ANOVA). While FPP (10 μM) had no effect on basal STAT6 phosphorylation, FPP augmented IL13-induced p-STAT6 by 1.53-fold (IL13 vs. IL13+FPP, *p<0.05 by 1-way ANOVA).

(D) In untreated control cells, Ras was predominantly in the cytosol (*p<0.05 by 2-way ANOVA) whereas treatment with FPP (10 μM), IL13, or IL13+FPP caused a relative

increase in membrane Ras with a complementary decrease in cytosolic Ras (**p<0.0001 by 2-way ANOVA) as compared to the control group ($^{f,\Phi}$ p=0.0043 by 1-way ANOVA). There was no significant difference in Ras localization between IL13 and IL13+FPP. Membrane (E-cadherin) and cytosolic (GAPDH) loading controls indicate appropriate separations for [C] and [M] subcellular fractions for Ras protein comparisons.

(E) In untreated control cells, Ras was predominantly in the cytosol (*p<0.05 by 2-way ANOVA) whereas treatment with FTI (20 μM) and IL13 independently caused a relative increase in membrane Ras and decrease in cytosolic Ras (**p<0.01 by 2-way ANOVA) as compared to the control group ($^{f,\Phi}$p=0.0385 by 1-way ANOVA for IL13 only, p=NS for FTI). There was no statistically significant difference between IL13 and IL13+FTI. Membrane (E-cadherin) and cytosolic (GAPDH) loading controls indicate appropriate separations for [C] and [M] subcellular fractions for Ras protein comparisons.

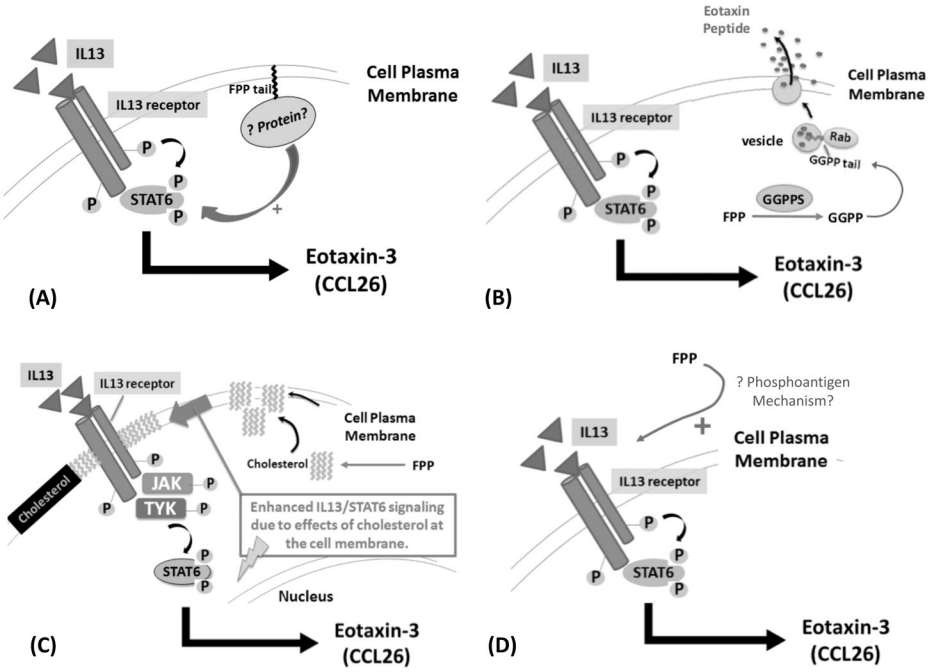

Figure 11. Hypothetical Mechanisms of How FPP Could Augment IL13-Mediated Signaling in Human Airway Epithelial Cells

Adding FPP exogenously to HBE1 cells caused a marked and unexpected increase in IL13-mediated STAT6 activation resulting in greater eotaxin-3 extracellular peptide secretion. The mechanism underlying this dramatic effect of FPP is not known. We propose four potential mechanisms that can be explored in forthcoming experiments to elucidate this important observation.

(A) Increased farnesylation of a protein with the CaaX- motif by FTase which then enhances IL13-mediated STAT6 phosphorylation and subsequent eotaxin-3 production.

(B) FPP is converted to GGPP by geranylgeranylpyrophosphate synthase (GGPPS) which then geranylgeranylates Rab GTPases to promote vesicular secretion (or exocytosis) of eotaxin-3 peptide.

(C) FPP is metabolized to squalene then to cholesterol which enhances cell plasma membrane rigidity via increased lipid microdomains/rafts, and subsequent enhanced IL13 receptor/IL13 ligand stability, leading to augmented IL13 signaling and greater eotaxin-3 production.

(D) FPP acts like a *phosphoantigen* via the butyrophilin receptor family to augment IL13-mediated STAT6 phosphorylation and eotaxin-3 production in bronchial epithelial cells.